



LJMU Research Online

Thull, S, Neacsu, C, O'Reilly, AO, Bothe, S, Hausmann, R, Huth, T, Meents, J and Lampert, A

Mechanism underlying hooked resurgent-like tail currents induced by an insecticide in human cardiac Nav1.5.

<http://researchonline.ljmu.ac.uk/id/eprint/13045/>

Article

Citation (please note it is advisable to refer to the publisher's version if you intend to cite from this work)

Thull, S, Neacsu, C, O'Reilly, AO, Bothe, S, Hausmann, R, Huth, T, Meents, J and Lampert, A (2020) Mechanism underlying hooked resurgent-like tail currents induced by an insecticide in human cardiac Nav1.5. *Toxicology and Applied Pharmacology*. 397. ISSN 0041-008X

LJMU has developed **LJMU Research Online** for users to access the research output of the University more effectively. Copyright © and Moral Rights for the papers on this site are retained by the individual authors and/or other copyright owners. Users may download and/or print one copy of any article(s) in LJMU Research Online to facilitate their private study or for non-commercial research. You may not engage in further distribution of the material or use it for any profit-making activities or any commercial gain.

The version presented here may differ from the published version or from the version of the record. Please see the repository URL above for details on accessing the published version and note that access may require a subscription.

For more information please contact researchonline@ljmu.ac.uk

<http://researchonline.ljmu.ac.uk/>

1
2
3
4
5
6
7
8
9
10
11
12
13
14
15
16
17
18
19
20
21
22
23
24
25
26
27
28
29
30
31
32
33
34
35
36
37
38
39
40
41
42
43
44
45
46
47
48
49
50
51
52
53
54
55
56
57
58
59
60
61
62
63
64
65

2

Mechanism underlying hooked resurgent-like tail currents induced by an insecticide in human cardiac Nav1.5

Sarah Thull^a, Cristian Neacsu^b, Andrias O. O'Reilly^c, Stefanie Bothe^{a,d}, Ralf Hausmann^e, Tobias Huth^b,
Jannis Meents^{a*}, Angelika Lampert^{a,d,f*}

^aInstitute of Physiology, RWTH Aachen University, Pauwelsstr. 30, 52074 Aachen, Germany; ^bInstitut für Physiologie und Pathophysiologie, Friedrich-Alexander-Universität Erlangen-Nürnberg, Universitätsstr. 17, 91054 Erlangen, Germany; ^cSchool of Natural Sciences and Psychology, Liverpool John Moores University, Liverpool, UK, ^dResearch Training Group 2416 MultiSenses-MultiScales, RWTH Aachen University, Aachen, Germany, ^eInstitute of Clinical Pharmacology, RWTH Aachen University, Wendlingweg 2, 52074 Aachen, Germany, ^fResearch Training Group 2415 ME3T, RWTH Aachen University, Aachen, Germany

* shared corresponding authors

Manuscript correspondence:

Angelika Lampert

Institute of Physiology, RWTH Aachen University, Pauwelsstr. 30, 52074 Aachen, Germany

E-mail: alampert@ukaachen.de

Tel: +49 (0) 241 80-88811

Fax: +49 (0) 241 80-82434

1 **Abstract**

2 Voltage-gated sodium channels are responsible not only for the fast upstroke of the action potential,
3 but they also modify cellular excitability via persistent and resurgent currents. Insecticides act via
4 permanently opening sodium channels to immobilize the animals. Cellular recordings performed
5 decades ago revealed distinctly hooked tail currents induced by these compounds. Here, we applied
6 the classical type-II pyrethroid deltamethrin on human cardiac Nav1.5 and observed resurgent-like
7 currents at very negative potentials in the absence of any pore-blocker, which resemble those hooked
8 tail currents. We show that deltamethrin dramatically slows both fast inactivation and deactivation of
9 Nav1.5 and thereby induces large persistent currents. Using the sea anemone toxin ATx-II as a tool to
10 prevent all inactivation-related processes, resurgent-like currents were eliminated while persistent
11 currents were preserved. Our experiments suggest that, in deltamethrin-modified channels, recovery
12 from inactivation occurs faster than delayed deactivation, opening a brief window for sodium influx
13 and leading to hooked, resurgent-like currents, in the absence of an open channel blocker. Thus, we
14 now explain with pharmacological methods the biophysical gating changes underlying the
15 deltamethrin induced hooked tail currents.

16 **Key words**

17 Voltage-gated sodium channel, human Nav1.5, sodium channel gating states, resurgent current,
18 pyrethroid, deltamethrin

19 **Summary**

20 The pyrethroid deltamethrin induces hooked resurgent-like tail currents in human cardiac voltage-
21 gated Nav1.5 channels. Using deltamethrin and ATx-II, we identify additional conducting channel
22 states caused by a faster recovery from inactivation compared to the deltamethrin-induced delayed
23 deactivation.

24

1 Introduction

2 Voltage-gated sodium (Nav) channels consist of four homologous domains (DI – IV), each with six
3 transmembrane segments (S1 – 6), that form the α -subunit (Ahern et al., 2016; Catterall, 2000). They
4 are responsible for the fast upstroke of the action potential. The insecticide class of pyrethroids has
5 been used abundantly since the 1970s, combatting agricultural pests and disease vectors, such as the
6 malaria-transmitting *anopheles* mosquito (Field et al., 2017). Pyrethroids affect the function of insect
7 Nav channels: They mostly act by slowing deactivation, thus keeping the channels open and disrupting
8 the electrical communication of insect nerves and muscle cells (Soderlund, 2010, 2012). Already
9 decades ago, these compounds were investigated in patch-clamp recordings and described to induce
10 the so-called “hooked tail currents”: during repolarization following a depolarizing voltage step the
11 channels would reactivate, and thereby form a typical hook, instead of the normally visible single
12 exponential decline of the tail currents (Tatebayashi and Narahashi, 1994; Song and Narahashi, 1996).
13 It was speculated about the underlying molecular mechanism, but to date it was not resolved.

14 Following depolarization, Nav channels activate due to outward movement of the voltage-sensors of
15 each domain (Chahine et al., 1994; Yang et al., 1996; Ahern, 2013). Milliseconds after activation, and
16 after the four channel domains have moved to their outward position, the inactivation particle (located
17 within the linker between DIII and DIV) binds to the open pore most likely from the transmembranal
18 side, as suggested by an allosterical model (Yan et al., 2017; Pan et al., 2018; Rühlmann et al., 2019):
19 this induces a conformational change which occludes the permeation pathway (Bezanilla and
20 Armstrong, 1977; Armstrong, 1981; West et al., 1992; Catterall, 2000; Armstrong, 2006). During
21 repolarization, the four activated domains return to their resting position, thus closing the channel pore
22 and deactivating the channel (Kuo and Bean, 1994). Recent models of Nav channel gating suggest that
23 activation of DI – III is sufficient for channel opening and current flux. DIV movement, albeit not
24 required for channel opening, is responsible for initiating fast inactivation as it forms the docking site
25 of the inactivation particle. Equally, the return of DIV to its resting position is required for the
26 detachment of the inactivation particle and recovery of the channel from fast inactivation (Kuo and
27 Bean, 1994; Armstrong, 2006; Capes et al., 2013; Ahern et al., 2016). Pyrethroids are mainly predicted

1 to bind to DII and DIII S6 of the insect Nav channel (Vais et al., 2003; O'Reilly et al., 2006;
2 Usherwood et al., 2007; Oliveira et al., 2013; Dong et al., 2014; Du et al., 2015), thus stabilizing the
3 bound channel domain, most probably DII, in its activated conformation. Accordingly, deltamethrin
4 has been shown to impair the transition of DII to its deactivated position (O'Reilly et al., 2006;
5 Oliveira et al., 2013; Dong et al., 2014; O'Reilly et al., 2014; Du et al., 2015). Thus, deltamethrin
6 mainly affects Nav channels by slowing of deactivation (Tabarean and Narahashi, 1998, 2001; Vais et
7 al., 2000) but might also have a minor effect on fast inactivation (Chinn and Narahashi, 1986; He and
8 Soderlund, 2016; James et al., 2017).

9 Although humans are less sensitive to pyrethroids, neurotoxic symptoms of pyrethroid intoxication
10 have been described and are most likely mediated by Nav modification (Mowry et al., 2016; Field et
11 al., 2017; James et al., 2017). They include T-syndrome (tremor) for type-I pyrethroids and CS-
12 syndrome (choreoathetosis and salivation) for type-II pyrethroids, including deltamethrin. Besides
13 these common neuronal symptoms after pyrethroid intoxication, some case studies of human
14 deltamethrin intoxication report of chest tightness and palpitations, pointing towards potential cardiac
15 side effects of the pyrethroid (He et al., 1989; Mowry et al., 2016).

16 Nine Nav channel α -subunits (Nav1.1 – 1.9) have been identified to date (Catterall, 2000; Ahern et al.,
17 2016). The main Nav channel in cardiac tissue is Nav1.5 and mutations of this channel are known to
18 cause cardiac diseases, such as long QT syndrome type 3, Brugada syndrome or sick sinus syndrome
19 (Zaydman et al., 2012; Varga et al., 2015). Thus, deltamethrin at higher concentrations may induce
20 Nav1.5-mediated cardiac side effects in humans.

21 One or two smaller auxiliary sodium channel β -subunits (β 1- 4) may be associated with one Nav
22 channel α -subunit (Catterall, 2000, 2010), regulating different channel functions (Calhoun and Isom,
23 2014; Zhu et al., 2017). The β 4-subunit is most likely involved in the generation of resurgent currents:
24 during depolarization a positively charged intracellular pore-blocker, most likely the C-terminus of the
25 β 4-subunit (Lewis and Raman, 2014), may quickly enter and occlude the open pore. This open-
26 channel block impairs fast inactivation. Unbinding of the pore-blocker upon repolarization generates
27 the “resurgent current” (Raman and Bean, 1997; Lewis and Raman, 2014). This classical resurgent

1 current is believed to promote high-frequency action potential firing (Raman and Bean, 1997, 2001)
2 but is also linked to certain disease states e.g. paroxysmal extreme pain disorder (Jarecki et al., 2010;
3 Hampl et al., 2016) or epilepsy (Hargus et al., 2013).

4 The sea anemone toxin ATx-II profoundly enhances persistent currents and classical resurgent
5 currents induced by the β 4-peptide (Klinger et al., 2012; Lewis and Raman, 2013). The toxin impairs
6 fast inactivation by slowing the outward movement of DIV, keeping it in its resting position (el-Sherif
7 et al., 1992; Warmke et al., 1997; Sheets et al., 1999; Vais et al., 2000; Stevens et al., 2011). These
8 properties render this toxin a handy tool to study the involvement of DIV movement in sodium
9 channel gating.

10 Using these tools, we here describe the molecular mechanism underlying hooked tail currents induced
11 by pyrethroids: Deltamethrin provokes resurgent-like sodium current at very negative potentials in the
12 absence of an open channel blocker. Using both deltamethrin, which slows deactivation (e.g. of DII),
13 and ATx-II, which slows activation of DIV, we identify an additional conducting sodium channel
14 gating state that resembles resurgent currents, underlying the so-called “hooked tail currents”. We
15 present a model that explains the effects of both compounds on Nav1.5 function and give evidence for
16 an alternative way of resurgent current induction in sodium channels.

17 **Experimental Procedures**

18 **Cell culture and transfection**

19 HEK293 cells, either stably expressing human Nav1.5 or used for transient transfection of Nav1.7,
20 were maintained in DMEM/ F-12 medium (Gibco-Life technologies) including 10% FBS, 1%
21 Penicillin/Streptomycin (A&E Scientific). 0.1mg/ml Zeocin (Thermo Fischer Scientific) was added to
22 the medium for the HEK293 cell line stably expressing human Nav1.5. ND7 cells used for transient
23 transfection with Nav1.8 were maintained in DMEM/ F-12 medium (Gibco-Life technologies) with a
24 higher glucose rate of 4.5 g/l, including 10% FBS. Cells were incubated at 37 °C and 5% CO₂.

25 Human Nav1.8 plasmid in a modified pIRESpuro3 vector (Kaluza et al., 2018) and human Nav1.7
26 plasmid in a pCMV6-neo vector (Klugbauer et al., 1995; Stadler et al., 2015) were transfected using

1 JetPEI reagent (Polyplus Transfection, Illkirch, France): 1.375 µg Nav1.7/ Nav1.8 WT DNA was
2 transfected to HEK293 cells for Nav1.7 and to ND7 cells for Nav1.8, using 3 µl of the JetPEI reagent.
3
4 The channel constructs were cotransfected with 0.125 µg GFP to detect transfected cells via green
5
6 fluorescence. Cells were recorded one day after transfection.
7
8

9 **Chemicals**

10 All chemicals were purchased from Sigma (Germany) or Merck (Germany) unless otherwise stated. A
11
12 stock solution of the β4-peptide (sequence 'KKLITFILKKTREK', PSL GmbH), dissolved in water,
13
14 was diluted in internal solution to a final concentration of 100 µM and kept at 4°C until used for
15
16 experiments.
17
18

19
20
21 Recombinant ATx-II (Anemonia sulcata toxin, Alomone Labs, Jerusalem, Israel or Sigma-Aldrich,
22
23 USA), dissolved in water, was added to the bath solution to a final concentration of 5 nM.
24

25
26 Deltamethrin (Sigma-Aldrich, USA), diluted in DMSO, was added to the bath solution to a final
27
28 concentration of 1 µM. The final concentration of DMSO in extracellular solution for recordings of
29
30 Nav1.5 did not exceed 0.1% or 0.2% for Nav1.7 and Nav1.8, which had no effect on sodium currents.
31
32 In control recordings, cells were treated with a vehicle (0.1% DMSO, or 0.2% for Nav1.7 and Nav1.8)
33
34 in bath solution, instead of deltamethrin or ATx-II. Cells treated with vehicle and HEK293 cells
35
36 expressing Nav1.5 treated with deltamethrin were incubated for minimum 5 min before each recording
37
38 in the same dish as they were patched. HEK293 cells transfected with Nav1.7 and ND7 cells
39
40 transfected with Nav1.8 treated with deltamethrin were patched on coverslips coated with PDL (Poly-
41
42 D-Lysine Hydrobromide (Sigma-Aldrich, USA)) and transferred to a dish pre-incubated with
43
44 deltamethrin for minimum 5 min.
45
46
47
48

49 **Electrophysiology**

50
51 Whole-cell patch-clamp experiments on HEK293 cells, stably expressing human Nav1.5, were
52
53 performed with an EPC-10USB amplifier (HEKA Elektronik, Lambrecht, Germany) at room
54
55 temperature. Glass pipettes, manufactured with a DMZ puller (Zeitz Instruments GmbH, Martinsried,
56
57 Germany) to a resistance of 0.9 to 2.5 MOhm were filled with internal solution containing (in mM):
58
59 140 CsF, 10 NaCl, 10 HEPES, 1 EGTA, 18 Sucrose (pH 7.33, adjusted with CsOH). For some
60
61
62
63
64
65

1 experiments β 4-peptide was diluted in internal solution to a final concentration of 100 μ M. The
 2 external bath solution contained (in mM): 140 NaCl, 3 KCl, 1 MgCl₂, 1 CaCl₂, 10 HEPES, 20 Glucose
 3 (pH 7.4, adjusted with NaOH).

4 Capacitive transients were cancelled and series resistance (≤ 5 MOhm, for measurements of the
 5 recovery of fast inactivation and for recordings with 10 μ M deltamethrin ≤ 7 MOhm) was
 6 compensated by at least 65%. Leak current was subtracted online using the P/4 procedure following
 7 (Nav1.5) or preceding (Nav1.7 and Nav1.8) the test pulse. Signals were digitized at sampling rates of
 8 100 kHz for recordings of current-voltage relations, steady-state fast inactivation and deactivation and
 9 50 kHz for recordings of resurgent current and recovery of fast inactivation. Low-pass filter frequency
 10 was set to 10 kHz. Voltage protocols were started 3 to 5 min after establishing the whole-cell
 11 configuration to allow for current stabilization. The holding potential was set to -120mV, except for
 12 measurements of recovery of fast inactivation of Nav1.5 with deltamethrin, where a holding potential
 13 of -150mV was used to avoid a time-dependent shift of fast inactivation. For acquisition and off-line
 14 analysis Patchmaster/ Fitmaster software (HEKA Elektronik, Lamprecht, Germany) was used.
 15 Currents of activation, steady-state fast inactivation, decay of fast inactivation, deactivation and
 16 recovery of fast inactivation curves as well as persistent current were analyzed without leak
 17 subtraction to reduce the impact of deltamethrin-altered leak currents on Nav1.5 sodium currents. The
 18 above-mentioned currents were additionally analyzed without zero offset subtraction to include
 19 persistent current summation during protocol repetition.

20 Current-voltage (I-V) relations were obtained using 100 ms pulses to a range of test potentials in
 21 10 mV steps at an interval of 5 seconds. The voltage-dependent sodium channel conductance G_{Na} was
 22 calculated using the following equation: $G_{Na} = I_{Na} / (V_m - V_{rev})$ where I_{Na} is the amplitude of the current
 23 at the voltage V_m , and V_{rev} is the reversal potential for sodium, which was determined for each cell
 24 individually. Conductance was normalized to the maximum conductance of each individual cell.

25 Activation curves were then derived by plotting normalized conductance ($G_{Na} / G_{Na,max}$) as a function of
 26 test potential and fitted with the Boltzmann equation: $G_{Na} / G_{Na,max} = G_{Na,max} / (1 + \exp [(V_m - V_{1/2}) / k])$

1 where $G_{Na, max}$ is the maximum sodium conductance, $V_{1/2}$ is the membrane potential at half-maximal
 2 channel activation, V_m is the membrane voltage and k is the slope factor.

3 Mean persistent current was evaluated after the first 100ms and during the final 10 ms of a 500 ms
 4 depolarizing pulse in a voltage range of -150mV to +20mV (in Fig. 4d) as well as during the final 13
 5 ms of a 100ms depolarizing pulse from -120mV to +20mV (see Fig. 2b (Thull et al., 2020)). Currents
 6 were normalized to the maximum current, elicited by the depolarizing pre-pulse.

7 Resurgent currents were assessed using a 20 ms depolarizing pre-pulse to 0 mV to allow channel
 8 opening, followed by a 500 ms test pulse in steps of 10 mV (ranging from -120 mV to +20 mV) with
 9 deltamethrin in the bath and in some experiments with the β 4-peptide in the internal solution or ATx-II
 10 in the external solution. Currents measured with β 4-peptide shown in Fig. 3d were assessed using a 20
 11 ms depolarizing pre-pulse to +30 mV, followed by 500 ms test pulses ranging from -120 mV to +20
 12 mV, as β 4-resurgent currents enhance with increasing depolarizations. To measure even very small
 13 resurgent currents, currents were analyzed without leak subtraction. Absolute currents were analyzed
 14 by subtracting the maximum resurgent current from a baseline which was defined as shown in Fig. 2a.
 15 Resurgent currents were normalized to the maximum inward current, elicited by the depolarizing pre-
 16 pulse. Resurgent current kinetics was investigated by measuring the time-to-peak of the resurgent
 17 current at the beginning of the repolarizing pulse.

18 Voltage-dependence of steady-state fast inactivation was measured using a series of 500 ms pre-pulses
 19 ranging from -150 mV to -10 mV in steps of 10 mV, followed by a 40 ms depolarization to +20 mV
 20 that served as a test pulse to assess the available non-inactivated channels. Normalized maximum
 21 inward current amplitude ($I_{Na}/I_{Na, Max}$) at each test pulse is displayed as a function of pre-pulse
 22 potential. Steady-state fast inactivation of vehicle recordings of Nav1.5 channels were fitted using the
 23 above Boltzmann equation, providing a measure of $V_{1/2}$ (the potential of half maximal inactivation).

24 For calculating the slow time course of persistent current decay, the above steady-state fast
 25 inactivation protocol was used to activate and inactivate channels. Only the slow component of current
 26 decay over 500 ms was fitted by a double-exponential equation (see Fig. 5a): $Y=Y_0+A_{fast}*\exp(-$

1 $K_{fast} * X) + A_{slow} * \exp(-K_{slow} * X)$, where Y_0 is the current amplitude at steady-state (i.e. plateau), A_{fast} and
 2 A_{slow} represent the amplitude coefficient for the fast and the slow time constants, K_{fast} and K_{slow}
 3 represent the two rate constants and X is the time. The time constants τ_{fast} and τ_{slow} are the reciprocals
 4 of the respective rate constant K .

5 For recovery experiments, channels were examined by using a 20 ms pre-pulse to -30 mV, followed
 6 by a repolarization to -110 mV for varying intervals (from 0.1 ms to 1638 ms) and a test-pulse to -30
 7 mV to determine the fraction of recovered channels. Test-pulse currents were normalized to the
 8 corresponding pre-pulse currents and plotted against recovery interval. The time constant of recovery
 9 of fast inactivation, given as τ , were calculated by fitting the data with a double-exponential equation
 10 as described above.

11 For deactivation experiments, channels were examined by using a 0.4 ms depolarizing pre-pulse to
 12 +20 mV, followed by a repolarization from -120 mV to +20 mV in 10 mV steps. For calculating the
 13 slow time course persistent current decay at deactivating voltages, the slow component of tail current
 14 decay over 100 ms was fitted by the above double-exponential equation (see Fig. 5b).

15 **Data analysis and statistics**

16 Data were analyzed and graphed using Fitmaster software (HEKA Elektronik), Igor Pro 5.2 and 6.3
 17 software (Wavemetrics), Graphpad Prism 5, 6, 7 or 8 (GraphPad Software) and Corel Draw X3–X6
 18 (Corel Corporation). Data are presented as mean \pm SEM.

19 For statistical testing, more than two groups were compared by an ANOVA or a Kruskal-Wallis test in
 20 case of non-Gaussian distribution, followed by a Bonferroni, Dunnett or Dunn post-hoc analysis. Two
 21 groups were compared with a student's t-test for parametric testing or a Mann Whitney test for non-
 22 parametric testing and significance was assumed if $p \leq 0.05$. We specified the significance level by the
 23 95% confidence interval, the difference between the means and t-ratio (difference between sample
 24 means divided by the standard error of the difference) for parametric testing or the actual difference
 25 between medians and the 95.10%, 95.69 % or 95.74% confidence interval (see Fig. 2 (Thull et al.,
 26 2020)) for non-parametric testing. Exponential fits and area under the curve (AUC) data were tested

- 1 for significant outliers with Grubb`s test (Graph pad QuickCalcs) and significant outliers were
- 2 excluded from analysis.

1
2
3
4
5
6
7
8
9
10
11
12
13
14
15
16
17
18
19
20
21
22
23
24
25
26
27
28
29
30
31
32
33
34
35
36
37
38
39
40
41
42
43
44
45
46
47
48
49
50
51
52
53
54
55
56
57
58
59
60
61
62
63
64
65

1 **Results**

2 **Deltamethrin induces resurgent-like currents without open-channel pore-blocker**

3 Nav channels may produce resurgent currents that are usually induced by an open-channel pore-
 4 blocker such as the β 4-peptide that unbinds during repolarization (Raman and Bean, 1997). Previous
 5 reports suggest that pyrethroids induce hooked tail currents (Tatebayashi and Narahashi, 1994; Song
 6 and Narahashi, 1996), and we tested whether deltamethrin has this effect on the neuronal sodium
 7 channels Nav1.7 and Nav1.8 and the cardiac sodium channel Nav1.5. Indeed, following incubation
 8 with 1 μ M deltamethrin, we observed hooked tail currents during a repolarization to -120 mV in all
 9 three channel isoforms (Fig. 1a, b and Fig. 2a, b). Nav1.7's sodium tail currents and their hook elicited
 10 by deltamethrin were small and hard to investigate (Fig. 1a), which is expected as mammalian Nav1.7
 11 is regarded as pyrethroid resistant (Tan and Soderlund, 2011). Hooked Nav1.8 tail currents induced by
 12 deltamethrin merged almost immediately into large and slow tail currents due to the slow gating
 13 properties of these channels and thus, complicated a decent analysis of the hooked tail currents (Fig.
 14 1b). We focused on investigating the hooked tail current component of Nav1.5 channels, as they are
 15 gating fast and evoke tail currents that were large enough and suitable for evaluating their hook and its
 16 underlying mechanism appropriately.

17 We investigated the effect of β 4-peptide on Nav1.5 channels with and without deltamethrin incubation
 18 in order to examine possible functional interactions between deltamethrin and β 4-peptide. β 4-induced
 19 resurgent currents arose between -60 mV and -30 mV (Fig. 3a, b). Deltamethrin-induced hooked,
 20 resurgent-like currents, on the other hand, had a different voltage dependence (between -120 mV and -
 21 90 mV, Fig. 2b), were approximately tenfold smaller (compare Fig. 2b and 3b) and slower to reach
 22 their peak (Fig. 3d) than those mediated by β 4. These data indicate that β 4-peptide and deltamethrin
 23 generate resurgent currents by distinct underlying processes.

24 Combining both, deltamethrin and β 4-peptide, resulted in approximately tenfold larger hooked,
 25 resurgent-like currents than those produced by deltamethrin alone (Fig. 3c). Interestingly, these
 26 currents now occurred almost over the entire voltage range from -120 mV to -10 mV, thus being a
 27 combination of deltamethrin and β 4-induced resurgent currents. When compared to the effect of

1 deltamethrin alone, currents induced by the combination of both compounds were slower to reach their
2 peak (Fig. 3d). These findings support the idea that two different mechanisms of deltamethrin and β 4-
3 peptide exist and can work synergistically to induce resurgent currents.

4 **Deltamethrin produces persistent current**

5 We investigated if deltamethrin affects voltage sensitivity of activation and fast inactivation of
6 Nav1.5. First, using a stepwise depolarization protocol (Fig. 4a), we found that 1 μ M deltamethrin did
7 not shift the activation midpoint of Nav1.5 in a hyperpolarized direction (Fig. 4a, b). Next, using a
8 two-pulse protocol (Fig. 4c) we found that steady-state fast inactivation of deltamethrin and of vehicle
9 measurements of Nav1.5 channels were identical (Fig. 4d), indicating that the voltage dependence of
10 steady-state fast inactivation is not affected by 1 μ M deltamethrin. However, Nav1.5 channels treated
11 with deltamethrin showed an unusual increase in relative current between -70 mV to -10 mV (Fig. 4d).
12 This increase seemed to correlate with a prominent persistent current, which we set out to analyze in
13 more detail.

14 Nav channels affected by deltamethrin are known to produce a continuous, persistent sodium inward
15 current that still flows after hundreds of milliseconds (James et al., 2017). While Nav1.5 channels did
16 not show any persistent current in vehicle measurements, deltamethrin-treated channels displayed
17 large persistent currents (Fig. 4a, c). However, these recordings also displayed a quickly inactivating
18 current component within the first milliseconds of depolarization. Thus, deltamethrin recordings seem
19 to expose two differently acting fractions of channels. The voltage dependence of persistent currents is
20 displayed in Fig. 4d. These currents only appear above -80 mV, which is the threshold of channel
21 opening (Fig. 4b), and reached up to 68% of transient current amplitude after 100 ms of
22 depolarization, decreasing to 32% of transient current amplitude after 500 ms of depolarization (Fig.
23 4d). This indicates that persistent currents have a very slow time course and that channels only fully
24 recover within the range of seconds.

25 In summary, the above data show that a fraction of channels seems to undergo regular gating and
26 appears to be unaffected by deltamethrin. These channels are presumably unbound by the insecticide.
27 Persistent current on the other hand seems to occur when a channel has bound deltamethrin. These

1 channels remain continuously permeable to sodium ions and hence escape analysis to some extent due
2 to their extremely altered gating kinetics. Deltamethrin presumably slows the time constants of fast
3 inactivation and of deactivation and increases the likelihood to adopt an open state. Next, we therefore
4 investigated the extremely slow time course of persistent currents and the effect of deltamethrin on
5 channel inactivation and deactivation kinetics.

6 **Deltamethrin slows fast inactivation and deactivation of a deltamethrin-bound Nav1.5** 7 **channel fraction.**

8 It has previously been suggested that deltamethrin mainly alters the deactivation process of Nav
9 channels (Tabarean and Narahashi, 1998, 2001; Vais et al., 2000). Accordingly, when applying a
10 voltage protocol for deactivation, we find large persistent currents even at very negative membrane
11 potentials (Fig. 5b, c). However, the large persistent currents that we observed during protocols for
12 fast inactivation (Fig. 4c), also suggest an effect of the compound on fast inactivation kinetics. Here,
13 we tried to quantify the slowing of inactivation and deactivation kinetics by deltamethrin.

14 First, we investigated gating kinetics of the presumably unbound channel fraction using protocols for
15 fast inactivation or channel deactivation (see Fig. 2 (Thull et al., 2020)). As expected, the fast time
16 constants of both gating mechanisms were unaltered in this channel fraction.

17 In order to investigate the very slow time course of persistent current decay and thereby the
18 deltamethrin-bound channels, we excluded the fast gating current component from our analysis and
19 only fit the slow persistent current with a double exponential function. This analysis could only be
20 performed in deltamethrin recordings, not in vehicle measurements, as the latter did not display any
21 persistent current that could be fitted. Persistent currents in fast inactivation protocols decayed with
22 slow time constants in the range of 200-400 ms (Fig. 5a), which corresponds with our earlier findings
23 that 32% channels are still conductive after 500 ms of depolarization (Fig. 4c, d). When we measured
24 channel deactivation, we found that deltamethrin-bound channels only deactivated with a very slow
25 time constant in the range of 100-200 ms, resulting in very slowly inactivating persistent currents (Fig.
26 5b). After 100 ms, 9 % of channels are still conductive even at -120 mV (Fig. 5c). These data
27 demonstrate that deltamethrin slows both fast inactivation and deactivation of Nav1.5 channels and

1 that these channels need hundreds of milliseconds to recover from the compound even at resting
2 voltages. However, it is not yet clear how the slowed deactivation and inactivation can lead to the
3 hooked, resurgent-like currents observed under deltamethrin treatment.

4 **Deltamethrin does not alter recovery of fast inactivation.**

5 In the case of conventional resurgent currents, the β 4-peptide blocks the open channel upon
6 depolarization while competing with the fast inactivation particle. Consequently, it prevents fast
7 inactivation (Raman and Bean, 2001; Lewis and Raman, 2014). So far, we have shown that
8 deltamethrin generates hooked, resurgent-like currents by a different mechanism than the β 4-peptide
9 (different voltage dependence, see Fig. 3), presumably by affecting channel gating kinetics.

10 Here, we investigated if deltamethrin affects the recovery from fast inactivation of Nav1.5. If recovery
11 was unaffected while deactivation was extremely slowed, channels might become conductive again
12 during repolarization before deactivating, thus producing small hooked, resurgent-like currents. We
13 chose a recovery potential of -110 mV as we observed the largest resurgent-like currents at that
14 voltage (Fig. 2b). Data were best fitted with a double-exponential equation and both fast and slow
15 recovery rates (τ_{fast} and τ_{slow}) were unaffected by deltamethrin treatment (Fig. 5d, e). It should be
16 noted, however, that approximately 48% of Nav1.5 channels produced a persistent current that
17 impeded analysis at very short recovery intervals below 10 ms (Fig. 5d, inset). In conclusion, 1 μ M
18 deltamethrin does not appear to have an impact on the recovery of fast inactivation kinetics of Nav1.5
19 channels. This agrees with the fact that deltamethrin most likely binds to DII whereas recovery from
20 fast inactivation is mediated by DIV movement (see Discussion).

21 **ATx-II prevents resurgent-like currents by deltamethrin**

22 So far, we have shown that deltamethrin slows deactivation and fast inactivation of Nav1.5 to produce
23 large persistent currents. At the same time, recovery from inactivation seems unaffected and this might
24 explain the observed hooked, resurgent-like currents. To confirm that the process of fast inactivation is
25 indeed necessary for resurgent-like currents, we chose the sea anemone toxin ATx-II as a tool to
26 completely abolish fast inactivation (el-Sherif et al., 1992; Lewis and Raman, 2013). ATx-II is
27 believed to stabilize DIV in its deactivated position, thus the inactivation-particle binding site is not

1 formed, and the toxin thereby impedes fast inactivation (el-Sherif et al., 1992; Warmke et al., 1997;
2 Vais et al., 2000). If fast inactivation is necessary for the hooked, resurgent-like currents induced by
3 deltamethrin, then ATx-II should prevent them.

4 The voltage dependence of Nav1.5 channel activation when treated with 0.5 nM ATx-II and 1 μ M
5 deltamethrin was similar to that recorded from untreated cells (see Fig. 3b (Thull et al., 2020)). In
6 comparison to deltamethrin alone, the combination of ATx-II and deltamethrin produced smaller
7 persistent currents but with the same voltage dependence (see Fig. 3c (Thull et al., 2020)). On the
8 other hand, the combination of ATx-II and β 4-peptide induced smaller persistent currents with a
9 different voltage dependence (see Fig. 3c (Thull et al., 2020)). This is consistent with different
10 underlying mechanisms: while ATx-II only inhibits fast inactivation, deltamethrin mainly inhibits
11 deactivation, which occurs at much more negative potentials.

12 The reduced persistent currents suggest that ATx-II can reduce the effect of deltamethrin on Nav1.5
13 gating. Accordingly, the combination of ATx-II and deltamethrin eliminated resurgent-like current
14 induction entirely, exclusively eliciting tail currents (Fig. 6a, b). It should be noted that binding sites
15 for deltamethrin and ATx-II do not overlap (Rogers et al., 1996; Vais et al., 2003; O'Reilly et al.,
16 2014), so a block of the deltamethrin binding site by ATx-II is unlikely (see Discussion). This suggests
17 that resurgent-like currents induced by deltamethrin indeed depend on functional fast inactivation,
18 which is impaired by ATx-II.

19 **Discussion**

20 The present study characterizes the effects of deltamethrin on human Nav1.5 channels. We show that
21 the pyrethroid slows deactivation and fast inactivation and stabilizes open channel states, not only
22 leading to persistent current but also to hooked, resurgent-like currents.

23 In order to explain these unusual currents, we propose a simplified Nav channel gating model (Fig. 7),
24 which is based on previous models (Kuo and Bean, 1994; Armstrong, 2006; Goldschen-Ohm et al.,
25 2013). The model visualizes the movement of the four Nav channel domains (DI to DIV) during
26 channel activation, inactivation and deactivation. During depolarization, in the absence of any

1 compound, Nav channel domains DI, DII and DIII quickly change their conformation to the outward
 2 position and activate successively. DIII moves first, followed simultaneously by DI and DII, leading to
 3 opening of the channel pore (Fig. 7 a, C1 – C4) (Chanda and Bezanilla, 2002; Armstrong, 2006). DIV
 4 moves last to complete voltage sensor movement (Fig. 7a, C4 to O). This last step allows the
 5 inactivation particle (IFM motif within DIII –IV linker) to block the open channel pore (Fig. 7a, I)
 6 (Bezanilla and Armstrong, 1977; West et al., 1992; Capes et al., 2013; Ahern et al., 2016). During
 7 repolarization of the cell membrane, the activated Nav channel domains DI and DII quickly return to
 8 their resting position, followed by DIII and DIV, thus, deactivating the channel (Fig. 7a, CI3 – CII)
 9 (Armstrong, 2006). Transition from state CII to state C1 involves the deactivation of DIV which
 10 finally allows the inactivation particle to unbind from the channel pore (Goldschen-Ohm et al., 2013).
 11 For the channel to be non-conductive, we assume that the channel pore either has to be blocked by the
 12 inactivation particle (Fig. 7a, I - CII) or at least one of the domains DI to DIII have to be in their
 13 deactivated resting position (Fig. 7a, C1 – C3) (Xiao et al., 2014). Accordingly, the only conducting
 14 channel states are C4 and O.

15 **Deltamethrin effect on Nav1.5 channel state properties**

16 Deltamethrin is supposed to bind to open states with a higher affinity (O'Reilly et al., 2006; McCavera
 17 and Soderlund, 2012). Still, it is known to marginally modify resting Nav channel states (Tan and
 18 Soderlund, 2010; James et al., 2017). Since the binding site for deltamethrin is predicted to be located
 19 at DII (DII S4-S5 linker, DII S5 and DII S6) (O'Reilly et al., 2006, 2014), we assume that
 20 deltamethrin mainly stabilizes DII in its activated position. When DII remains activated, the two
 21 activated states C3 and C4 become equivalent (Fig. 7b, C_{d3}/C_{d4}). Complete channel deactivation must
 22 be slowed if DII remains in its activated conformation. Indeed, our recordings show a slowed time
 23 constant of deactivation due to deltamethrin. Thus, our data correspond well with previous findings in
 24 insect and mammalian sodium channels and underline that deltamethrin slows channel deactivation
 25 (Tabarean and Narahashi, 1998; Vais et al., 2000; Tabarean and Narahashi, 2001). However, we also
 26 show a slowing of fast inactivation kinetics, producing large persistent currents.

1 **Hooked, resurgent-like currents**

2 To date the induction of resurgent currents has been believed to require the presence of an open-
 3 channel blocker, such as the short cytoplasmic C-terminus of the sodium channel β 4-subunit (Grieco
 4 et al., 2005). This peptide contains positively charged residues and is supposed to block open sodium
 5 channels from the intracellular side at positive voltages and unblock at negative potentials, while
 6 competing with fast inactivation (Lewis and Raman, 2014).

7 Contrary to the previously known β 4-peptide-induced resurgent currents, which occur at repolarizing
 8 voltages ranging from -70 mV to -30 mV, deltamethrin surprisingly produced hooked, resurgent-like
 9 currents at very negative potentials (-120 mV to -90 mV) (Fig. 2b). However, deltamethrin is not
 10 polar, unlike the β 4-peptide, whose polarity is believed to be crucial for open-channel block (Grieco et
 11 al., 2005; Lewis and Raman, 2011). Instead lipophilic pyrethroids are predicted to bind at a lipid-
 12 accessible transmembrane site on Nav channels (O'Reilly et al., 2006). This implies that deltamethrin
 13 induces hooked, resurgent-like currents by a distinct mechanism.

14 Generally, with deltamethrin binding to the channel at rest or during activation, two fractions of
 15 channels can be observed: a deltamethrin-bound fraction that produces large persistent currents (Fig.
 16 4) (James et al., 2017), and an unbound fraction that undergoes regular channel gating. The latter
 17 displays an unaffected voltage dependence of activation and steady-state fast inactivation as well as
 18 unchanged time constants of fast inactivation and deactivation.

19 We propose that hooked, resurgent-like currents are generated by a third, very small fraction of
 20 channels that bind deltamethrin *after* they have undergone fast inactivation (Fig. 7b): At very
 21 hyperpolarized potentials, the deactivation of DI-IV proceeds very quickly (Kuo and Bean, 1994;
 22 Armstrong, 2006; Lewis and Raman, 2014). Deltamethrin keeps DII in its activated position (Fig. 7b,
 23 C_d1), and thereby slows deactivation. In parallel, the channel will recover from fast inactivation at
 24 these negative potentials, which is mainly mediated by DIV movement to its deactivated position.
 25 Deactivation of DIV is believed to be rate-limiting for the inactivation particle to unbind from the
 26 channel pore (Kuo and Bean, 1994; Armstrong, 2006; Capes et al., 2013; Goldschen-Ohm et al., 2013;
 27 Ahern et al., 2016). With DII remaining in its outward position, recovery of fast inactivation becomes

1 faster than deactivation of DII. If DIV recovers before any of the other three domains, then the
 2 inactivation particle will unbind before the channel is fully closed by deactivation. The channel will
 3 therefore become conductive at these negative potentials (Fig. 7b, $I_d - C_{d3}/C_{d4}$; bold arrow), resulting
 4 in hooked, resurgent-like currents. If DI or DIII deactivate before DIV (Fig. 7b, transition $CI_{d2} - C_{d2}$
 5 or $CI_{d1} - C_{d1}$), no resurgent-like current can occur since a minimum of three domains has to be in the
 6 activated position for the channel to be conductive (Armstrong, 2006).

7 At more positive repolarization voltages, fast inactivation is favored and recovery from fast
 8 inactivation occurs slower. This would reduce the likelihood of DIV to deactivate before DI or DIII
 9 and channels therefore remain blocked by the inactivation particle until at least two channel domains
 10 return to their resting states (Kuo and Bean, 1994; Armstrong, 2006; Lewis and Raman, 2014). Under
 11 these circumstances, deltamethrin would not be able to induce resurgent-like currents at more positive
 12 voltages. These findings correspond well to our conclusion that resurgent-like current may arise when
 13 movement of at least one of the Nav channel domains I, II or III is altered.

14 **Additional permeable Nav channel gating states**

15 The finding that deltamethrin renders Nav channels conductive during hyperpolarized potentials and
 16 induces hooked, resurgent-like currents without an additional open-channel blocker, confirms two
 17 conclusions: First, DIV is able to deactivate before DI, DII and DIII. Second, channels with
 18 deactivated DIV are permeable to sodium current when recovery of fast inactivation happens before
 19 the other three domains are deactivated (Armstrong, 2006). Accordingly, Nav channels have to have
 20 more than only one conductive state, thus they can generate resurgent-like currents.

21 With deltamethrin stabilizing the activated DII, the total number of channel states in our simplified
 22 model is reduced from nine to seven (compare Fig. 7a to lower part of Fig. 7b). Thus, with
 23 deltamethrin the C_{d3}/C_{d4} state is reached quicker as there are only two closed states that precede this
 24 conductive state (Fig. 7b) and the probability to switch into one of the conductive states is increased.
 25 This is reflected in a slight shift of voltage dependence of activation to more hyperpolarized potentials
 26 by deltamethrin (Fig. 4b).

1 **ATx-II confirms additional permeable gating states**

2 ATx-II is thought to stabilize DIV in its deactivated conformation (Sheets et al., 1999; Stevens et al.,
3 2011), impairing open-state fast inactivation (Warmke et al., 1997; Vais et al., 2000). Closed-state
4 inactivation was first thought to be only marginally affected (el-Sherif et al., 1992). Yet, later results
5 have shown that ATx-II strongly impairs closed-state inactivation (Warmke et al., 1997).

6 Accordingly, by preventing DIV from activating and thus preventing the inactivation particle from
7 occluding the channel pore (Vais et al., 2000; Lewis and Raman, 2013), the amount of permeable
8 channel states is reduced to one (Fig. 7c). At the same time, closed-inactivated (CI) states, with the
9 fast inactivation particle blocking the channel pore, do not exist in this theoretical model. A fully
10 activated state (O) also does not exist, as DIV cannot activate. Accordingly, the only conductive state
11 is C4.

12 When ATx-II and deltamethrin are applied at the same time, the number of total channel states is
13 further reduced to three as C3 and C4 again become equivalent (Fig. 7d). The number of conducting
14 states remains one (C3/C4). This is in contrast to the situation with deltamethrin alone (Fig. 7b), where
15 there are two conducting states (C3/C4 and O).

16 ATx-II completely eliminated resurgent-like currents in Nav1.5 channels treated by deltamethrin. This
17 may have two reasons: binding of ATx-II and deltamethrin inhibit each other, or resurgent-like
18 currents depend on channel inactivation, which is abolished by ATx-II. While it is unlikely that the
19 binding of ATx-II prohibits additional binding of deltamethrin due to different binding sites (Rogers et
20 al., 1996; Vais et al., 2003; O'Reilly et al., 2014), we cannot fully exclude this possibility. However,
21 persistent currents during ATx-II plus deltamethrin treatment showed the same voltage dependence as
22 those with deltamethrin alone but different to those mediated by ATx-II with β 4-peptide (see Fig. 3c
23 (Thull et al., 2020)). Additionally, Nav channels affected by the triple combination of ATx-II, β 4-
24 peptide and deltamethrin present resurgent currents occurring from -120 mV to -10 mV (see Fig. 3e
25 (Thull et al., 2020)), which can only be explained by different binding sites and synergistically
26 working mechanisms of all three substances.

1 Since resurgent-like currents do not occur with ATx-II and since ATx-II prevents DIV activation, it
2 can be assumed that the movement of DIV is essential for hooked, resurgent-like currents. Following
3 this interpretation and our recent results, we can assume that with ATx-II and deltamethrin, the
4 inactivation particle does not bind to the channel pore (Fig. 7c, d) and therefore cannot unbind to allow
5 resurgent-like current. Thus, if ATx-II and deltamethrin are present, slowing of deactivation of DII by
6 deltamethrin does not suffice to produce resurgent-like currents.

7 **Physiological relevance**

8 A similar connection between recovery of fast inactivation through conductive channel states and
9 resurgent-like currents has been hypothesized earlier, with the observation of analogous currents
10 induced by the pyrethroid tetramethrin in rat Purkinje cells and dorsal root ganglia. These currents
11 have been described as “hooked tail currents” (Tatebayashi and Narahashi, 1994; Song and Narahashi,
12 1996). They have also been observed in adult frog muscle (Leibowitz et al., 1987) and were linked to a
13 β -scorpion toxin-induced negative-shift in activation of DIS4, DIIS4 and DIIS4 of different Nav
14 channel types (Cestèle et al., 1998; Schiavon et al., 2006, 2012). By deconstructing the different Nav
15 channel states contributing to hooked, resurgent-like currents induced by deltamethrin in fast gating
16 Nav1.5 channels, our results generally confirm this alternative mechanism of resurgent current
17 generation. These resurgent-like currents are primarily known to be caused by toxins that slow the
18 deactivation of Nav channel domain I, II or III.

19 Importantly, long-term studies have revealed that environmental exposure to pyrethroid insecticides is
20 linked to an increased risk of coronary heart disease and cardiovascular disease mortality (Han et al.,
21 2017; Bao et al., 2019). Accordingly, reports exist of chest tightness and palpitations after
22 deltamethrin intoxication (He et al., 1989; Mowry et al. 2016). Our data generally support the notion
23 of cardiac side effects due to deltamethrin and we provide a detailed investigation of the compound’s
24 effects on human cardiac Nav1.5 channels.

25 Following occupational dermal exposure, main adverse effects are paranessthesiae, most likely due to
26 hyperactivity of cutaneous sensory nerve fibres (Bradberry et al., 2005). Main symptoms of pyrethroid

1 poisoning are neurological since pyrethroids are known to pass through the blood-brain barrier due to
2 their lipophilicity (Bradberry et al., 2005; Godin et al., 2010). However, plasma protein binding limits
3 brain uptake of deltamethrin under physiological conditions, which adds further evidence to the low
4 acute CNS toxicity in humans in non-excessive exposures (Amaraneni et al., 2016), although chronic
5 long-term pyrethroid exposure seems to be associated with neurological deficits such as deteriorated
6 neurocognitive performance (Hansen et al., 2017). Hooked tail currents are not only present in cardiac
7 Nav1.5 channels but also in neuronal Nav channels such as Nav1.7 and Nav1.8. Deltamethrin also
8 affects β 4-mediated “conventional” resurgent currents. The combination of β 4-peptide and
9 deltamethrin involves two mechanisms working synergistically to produce enhanced, voltage-
10 independent resurgent currents: As deltamethrin is believed to stabilize the opened Nav channel pore,
11 it facilitates the β 4-peptide to find its way into the channel pore, even at very negative potentials.
12 Thus, intoxication effects mediated by neuronal Nav channels subtypes might be aggravated by these
13 two synergistically working mechanisms. Consequently, deltamethrin might also have an impact on
14 the firing behavior of cell types naturally producing resurgent currents such as purkinje cells (Raman
15 and Bean, 1997, 2001), in addition to the obvious, large persistent current induced by the compound.
16 Thus, we here uncovered the mechanism underlying those resurgent-like currents exemplarily in
17 Nav1.5 channels. Further investigations about resurgent-like currents in other neuronal Nav channel
18 subtypes such as Nav1.9 and their impact on Nav channel gating properties are essential and beneficial
19 to fully understand the pyrethroids’ effect on neuronal Nav channel subtypes, causing the prominent
20 and severe neuronal intoxication symptoms.

21 **Conclusion**

22 In summary, our data show that deltamethrin, a type-II pyrethroid, can induce hooked, resurgent-like
23 currents in the absence of a pore-blocker in human cardiac Nav1.5 channels. These currents are
24 generated by re-opening Nav1.5 channels, when they recover from fast inactivation before they
25 completely deactivate. By establishing a model of ATx-II and deltamethrin interaction with Nav
26 channels, we show that resurgent currents can be induced by slowing deactivation and thus by
27 disrupting the interaction between fast inactivation and deactivation of Nav channels. Our findings

1 highlight how Nav channel functions can be affected by even small disruptions of the sensitive
2 interplay of their different gating states. Our investigations of deltamethrin in human cardiac Nav1.5
3 channels characterize potential effects of pyrethroid exposure for humans and can provide a first
4 attempt in explaining cardiac symptoms induced by deltamethrin. Since pyrethroids are very common
5 insecticides, our results emphasize the importance of investigating their broad spectrum of effects on
6 human Nav channels in detail.

7 **Acknowledgements**

8 The authors thank Petra Hautvast and Brigitte Hoch for excellent technical assistance. The authors
9 declare no competing financial interests. This work was supported in part by the DFG LA 2740/3-1
10 and the DFG-funded research training groups 363055819/GRK2415 and 368482240/GRK2416 (all
11 to A.L.).

12 **Author contributions**

13 S.T. Investigation (lead). Data curation (lead). Formal analysis (lead). Verification. Visualization
14 (lead). Writing – original draft. Writing – review and editing.

15 C.N. Investigation. Data curation. Formal analysis. Visualization.

16 A.O.O. Writing – review and editing.

17 S.B. Data curation. Writing – review and editing.

18 R.H. Data curation. Writing – review and editing.

19 T.H. Writing – review and editing.

20 J.M. Conceptualization. Data curation. Formal analysis. Supervision. Visualization. Writing – review
21 and editing.

22 A.L. Conceptualization. Funding acquisition. Project administration. Resources. Supervision. Writing
23 – review and editing.

1 Related Article

- 2 Sarah Thull, Cristian Neacsu, Andrias O. O'Reilly, Stefanie Bothe, Ralf Hausmann, Tobias Huth,
3 Jannis Meents, Angelika Lampert. Dataset of electrophysiological patch-clamp recordings of the effect
4 of the compounds deltamethrin, ATx-II and β 4-peptide on human cardiac Nav1.5 channel gating
5 properties. 2020. *Data in Brief*. Under Review

6 Literature

- 7 Ahern, C.A. 2013. What activates inactivation? *J. Gen. Physiol.* 142:97–100.
8 doi:10.1085/jgp.201311046.
- 9 Ahern, C.A., J. Payandeh, F. Bosmans, and B. Chanda. 2016. The hitchhiker's guide to the voltage-
10 gated sodium channel galaxy. *J. Gen. Physiol.* 147:1–24. doi:10.1085/jgp.201511492.
- 11 Amaraneni, M., A. Sharma, J. Pang, S. Muralidhara, B.S. Cummings, C.A. White, J.V. Bruckner, and
12 J. Zastre. 2016. Plasma protein binding limits the blood brain barrier permeation of the
13 pyrethroid insecticide, deltamethrin. *Toxicol. Lett.* 250–251:21–28.
14 doi:10.1016/j.toxlet.2016.03.006.
- 15 Armstrong, C.M. 1981. Sodium channels and gating currents. *Physiol. Rev.* 61:644–683.
- 16 Armstrong, C.M. 2006. Na channel inactivation from open and closed states. *Proc. Natl. Acad. Sci. U.*
17 *S. A.* 103:17991–17996. doi:10.1073/pnas.0607603103.
- 18 Bao, W., B. Liu, D.W. Simonsen, and H.-J. Lehmler. 2019. Association Between Exposure to
19 Pyrethroid Insecticides and Risk of All-Cause and Cause-Specific Mortality in the General US
20 Adult Population. *JAMA Intern. Med.* doi:10.1001/jamainternmed.2019.6019.
- 21 Bezanilla, F., and C. Armstrong. 1977. Inactivation of the sodium channel. I. Sodium current
22 experiments. *J. Gen. Physiol.* 70:549–566.
- 23 Bradberry, S.M., S.A. Cage, A.T. Proudfoot, and J.A. Vale. 2005. Poisoning due to pyrethroids.
24 *Toxicol. Rev.* 24:93–106. doi:10.2165/00139709-200524020-00003.
- 25 Calhoun, J.D., and L.L. Isom. 2014. The role of non-pore-forming β subunits in physiology and
26 pathophysiology of voltage-gated sodium channels. *Handb. Exp. Pharmacol.* 221:51–89.
27 doi:10.1007/978-3-642-41588-3_4.
- 28 Capes, D.L., M.P. Goldschen-Ohm, M. Arcisio-Miranda, F. Bezanilla, and B. Chanda. 2013. Domain
29 IV voltage-sensor movement is both sufficient and rate limiting for fast inactivation in sodium
30 channels. *J. Gen. Physiol.* 142:101–112. doi:10.1085/jgp.201310998.
- 31 Catterall, W.A. 2000. From ionic currents to molecular mechanisms: the structure and function of
32 voltage-gated sodium channels. *Neuron.* 26:13–25.
- 33 Catterall, W.A. 2010. Ion Channel Voltage Sensors: Structure, Function, and Pathophysiology.
34 *Neuron.* 67:915–928. doi:10.1016/j.neuron.2010.08.021.

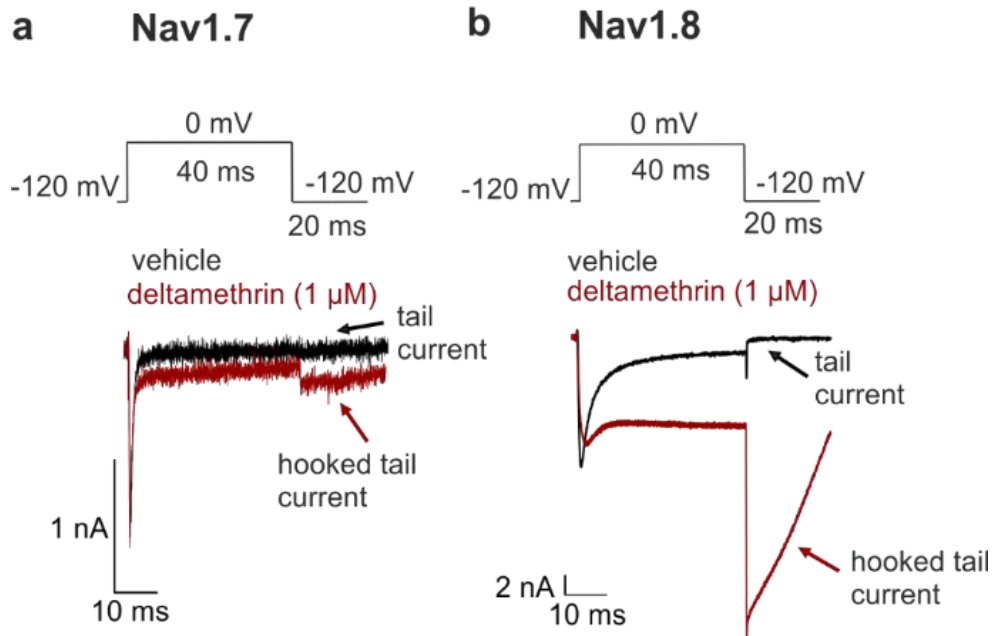
- 1 Cestèle, S., Y. Qu, J.C. Rogers, H. Rochat, T. Scheuer, and W.A. Catterall. 1998. Voltage sensor-
 2 trapping: enhanced activation of sodium channels by beta-scorpion toxin bound to the S3-S4
 3 loop in domain II. *Neuron*. 21:919–931.
- 4 Chahine, M., A.L. George, M. Zhou, S. Ji, W. Sun, R.L. Barchi, and R. Horn. 1994. Sodium channel
 5 mutations in paramyotonia congenita uncouple inactivation from activation. *Neuron*. 12:281–
 6 294. doi:10.1016/0896-6273(94)90271-2.
- 7 Chanda, B., and F. Bezanilla. 2002. Tracking voltage-dependent conformational changes in skeletal
 8 muscle sodium channel during activation. *J. Gen. Physiol.* 120:629–645.
- 9 Chinn, K., and T. Narahashi. 1986. Stabilization of sodium channel states by deltamethrin in mouse
 10 neuroblastoma cells. *J. Physiol.* 380:191–207. doi:10.1113/jphysiol.1986.sp016280.
- 11 Dong, K., Y. Du, F. Rinkevich, Y. Nomura, P. Xu, L. Wang, K. Silver, and B.S. Zhorov. 2014.
 12 Molecular Biology of Insect Sodium Channels and Pyrethroid Resistance. *Insect Biochem.*
 13 *Mol. Biol.* 50:1–17. doi:10.1016/j.ibmb.2014.03.012.
- 14 Du, Y., Y. Nomura, B.S. Zhorov, and K. Dong. 2015. Evidence for dual binding sites for DDT in
 15 Insect Sodium Channels. *J. Biol. Chem.* doi:10.1074/jbc.M115.678672.
- 16 Field, L.M., T.G. Emyr Davies, A.O. O’Reilly, M.S. Williamson, and B.A. Wallace. 2017. Voltage-
 17 gated sodium channels as targets for pyrethroid insecticides. *Eur. Biophys. J.* 46:675–679.
 18 doi:10.1007/s00249-016-1195-1.
- 19 Godin, S.J., M.J. DeVito, M.F. Hughes, D.G. Ross, E.J. Scollon, J.M. Starr, R.W. Setzer, R.B.
 20 Conolly, and R. Tornero-Velez. 2010. Physiologically based pharmacokinetic modeling of
 21 deltamethrin: development of a rat and human diffusion-limited model. *Toxicol. Sci. Off. J.*
 22 *Soc. Toxicol.* 115:330–343. doi:10.1093/toxsci/kfq051.
- 23 Goldschen-Ohm, M.P., D.L. Capes, K.M. Oelstrom, and B. Chanda. 2013. Multiple pore
 24 conformations driven by asynchronous movements of voltage sensors in a eukaryotic sodium
 25 channel. *Nat. Commun.* 4:1350. doi:10.1038/ncomms2356.
- 26 Grieco, T.M., J.D. Malhotra, C. Chen, L.L. Isom, and I.M. Raman. 2005. Open-channel block by the
 27 cytoplasmic tail of sodium channel beta4 as a mechanism for resurgent sodium current.
 28 *Neuron*. 45:233–244. doi:10.1016/j.neuron.2004.12.035.
- 29 Hampl, M., E. Eberhardt, A.O. O’Reilly, and A. Lampert. 2016. Sodium channel slow inactivation
 30 interferes with open channel block. *Sci. Rep.* 6:25974. doi:10.1038/srep25974.
- 31 Han, J., L. Zhou, M. Luo, Y. Liang, W. Zhao, P. Wang, Z. Zhou, and D. Liu. 2017. Nonoccupational
 32 Exposure to Pyrethroids and Risk of Coronary Heart Disease in the Chinese Population.
 33 *Environ. Sci. Technol.* 51:664–670. doi:10.1021/acs.est.6b05639.
- 34 Hansen, M.R.H., E. Jørs, F. Lander, G. Condarco, F. Debes, N. Tirado Bustillos, and V. Schlünssen.
 35 2017. Neurological Deficits After Long-term Pyrethroid Exposure. *Environ. Health Insights.*
 36 11. doi:10.1177/1178630217700628.
- 37 Hargus, N.J., A. Nigam, E.H. Bertram, and M.K. Patel. 2013. Evidence for a role of Nav1.6 in
 38 facilitating increases in neuronal hyperexcitability during epileptogenesis. *J. Neurophysiol.*
 39 110:1144–1157. doi:10.1152/jn.00383.2013.
- 40 He, B., and D.M. Soderlund. 2016. Effects of the β 1 Auxiliary Subunit on Modification of Rat Nav1.6
 41 Sodium Channels Expressed in HEK293 Cells by the Pyrethroid Insecticides Tefluthrin and
 42 Deltamethrin. *Toxicol. Appl. Pharmacol.* 291:58–69. doi:10.1016/j.taap.2015.12.007.

- 1 He, F., S. Wang, L. Liu, S. Chen, Z. Zhang, and J. Sun. 1989. Clinical manifestations and diagnosis of
2 acute pyrethroid poisoning. *Arch. Toxicol.* 63:54–58.
- 3 James, T.F., M.N. Nenov, C.M. Tapia, M. Lecchi, S. Koshy, T.A. Green, and F. Laezza. 2017.
4 Consequences of acute Nav1.1 exposure to deltamethrin. *Neurotoxicology.* 60:150–160.
5 doi:10.1016/j.neuro.2016.12.005.
- 6
7 Jarecki, B.W., A.D. Piekarz, J.O. Jackson, and T.R. Cummins. 2010. Human voltage-gated sodium
8 channel mutations that cause inherited neuronal and muscle channelopathies increase
9 resurgent sodium currents. *J. Clin. Invest.* 120:369–378. doi:10.1172/JCI40801.
- 10
11 Kaluza, L., J.E. Meents, M. Hampl, C. Rösseler, P.A.I. Hautvast, S. Detto-Dassen, R. Hausmann, G.
12 Schmalzing, and A. Lampert. 2018. Loss-of-function of Nav1.8/D1639N linked to human pain
13 can be rescued by lidocaine. *Pflüg. Arch. - Eur. J. Physiol.* 470:1787–1801.
14 doi:10.1007/s00424-018-2189-x.
- 15
16
17 Klinger, A.B., M. Eberhardt, A.S. Link, B. Namer, L.K. Kutsche, E.T. Schuy, R. Sittl, T. Hoffmann,
18 C. Alzheimer, T. Huth, R.W. Carr, and A. Lampert. 2012. Sea-anemone toxin ATX-II elicits
19 A-fiber-dependent pain and enhances resurgent and persistent sodium currents in large sensory
20 neurons. *Mol. Pain.* 8:69. doi:10.1186/1744-8069-8-69.
- 21
22
23 Klugbauer, N., L. Lacinova, V. Flockerzi, and F. Hofmann. 1995. Structure and functional expression
24 of a new member of the tetrodotoxin-sensitive voltage-activated sodium channel family from
25 human neuroendocrine cells. *EMBO J.* 14:1084–1090.
- 26
27 Kuo, C.-C., and B.P. Bean. 1994. Na⁺ channels must deactivate to recover from inactivation. *Neuron.*
28 12:819–829. doi:10.1016/0896-6273(94)90335-2.
- 29
30
31 Leibowitz, M.D., J.R. Schwarz, G. Holan, and B. Hille. 1987. Electrophysiological comparison of
32 insecticide and alkaloid agonists of Na channels. *J. Gen. Physiol.* 90:75–93.
- 33
34 Lewis, A.H., and I.M. Raman. 2011. Cross-species conservation of open-channel block by Na channel
35 β 4 peptides reveals structural features required for resurgent Na current. *J. Neurosci. Off. J.*
36 *Soc. Neurosci.* 31:11527–11536. doi:10.1523/JNEUROSCI.1428-11.2011.
- 37
38 Lewis, A.H., and I.M. Raman. 2013. Interactions among DIV voltage-sensor movement, fast
39 inactivation, and resurgent Na current induced by the Nav β 4 open-channel blocking peptide.
40 *J. Gen. Physiol.* 142:191–206. doi:10.1085/jgp.201310984.
- 41
42
43 Lewis, A.H., and I.M. Raman. 2014. Resurgent current of voltage-gated Na(+) channels. *J. Physiol.*
44 592:4825–4838. doi:10.1113/jphysiol.2014.277582.
- 45
46 McCavera, S.J., and D.M. Soderlund. 2012. Differential state-dependent modification of inactivation-
47 deficient Nav1.6 sodium channels by the pyrethroid insecticides S-bioallethrin, tefluthrin and
48 deltamethrin. *Neurotoxicology.* 33:384–390. doi:10.1016/j.neuro.2012.03.007.
- 49
50
51 Mowry, J.B., D.A. Spyker, D.E. Brooks, A. Zimmerman, and J.L. Schauben. 2016. 2015 Annual
52 Report of the American Association of Poison Control Centers' National Poison Data System
53 (NPDS): 33rd Annual Report. *Clin. Toxicol. Phila. Pa.* 54:924–1109.
54 doi:10.1080/15563650.2016.1245421.
- 55
56 Oliveira, E.E., Y. Du, Y. Nomura, and K. Dong. 2013. A residue in the transmembrane segment 6 of
57 domain I in insect and mammalian sodium channels regulate differential sensitivities to
58 pyrethroid insecticides. *Neurotoxicology.* 38:42–50. doi:10.1016/j.neuro.2013.06.001.
- 59
60
61
62
63
64
65

- 1 O'Reilly, A.O., B.P.S. Khambay, M.S. Williamson, L.M. Field, B.A. Wallace, and T.G.E. Davies.
2 2006. Modelling insecticide-binding sites in the voltage-gated sodium channel. *Biochem. J.*
3 396:255–263. doi:10.1042/BJ20051925.
- 4 O'Reilly, A.O., M.S. Williamson, J. González-Cabrera, A. Turberg, L.M. Field, B.A. Wallace, and
5 T.G.E. Davies. 2014. Predictive 3D modelling of the interactions of pyrethroids with the
6 voltage-gated sodium channels of ticks and mites. *Pest Manag. Sci.* 70:369–377.
7 doi:10.1002/ps.3561.
- 8 Pan, X., Z. Li, Q. Zhou, H. Shen, K. Wu, X. Huang, J. Chen, J. Zhang, X. Zhu, J. Lei, W. Xiong, H.
9 Gong, B. Xiao, and N. Yan. 2018. Structure of the human voltage-gated sodium channel
10 Nav1.4 in complex with β 1. *Science*. 362:eaau2486. doi:10.1126/science.aau2486.
- 11 Raman, I.M., and B.P. Bean. 1997. Resurgent sodium current and action potential formation in
12 dissociated cerebellar Purkinje neurons. *J. Neurosci. Off. J. Soc. Neurosci.* 17:4517–4526.
- 13 Raman, I.M., and B.P. Bean. 2001. Inactivation and recovery of sodium currents in cerebellar Purkinje
14 neurons: evidence for two mechanisms. *Biophys. J.* 80:729–737.
- 15 Rogers, J.C., Y. Qu, T.N. Tanada, T. Scheuer, and W.A. Catterall. 1996. Molecular determinants of
16 high affinity binding of alpha-scorpion toxin and sea anemone toxin in the S3-S4 extracellular
17 loop in domain IV of the Na⁺ channel alpha subunit. *J. Biol. Chem.* 271:15950–15962.
- 18 Rühlmann, A.H., J. Körner, N. Bebrivenski, S. Detro-Dassen, P. Hautvast, C.A. Benasolo, J. Meents,
19 J.-P. Machtens, G. Schmalzing, and A. Lampert. 2019. Uncoupling sodium channel dimers
20 rescues phenotype of pain-linked Nav1.7 mutation. *bioRxiv*. 716654. doi:10.1101/716654.
- 21 Schiavon, E., M. Pedraza-Escalona, G.B. Gurrola, T. Olamendi-Portugal, G. Corzo, E. Wanke, and
22 L.D. Possani. 2012. Negative-shift activation, current reduction and resurgent currents induced
23 by β -toxins from *Centruroides* scorpions in sodium channels. *Toxicon Off. J. Int. Soc.*
24 *Toxinology*. 59:283–293. doi:10.1016/j.toxicon.2011.12.003.
- 25 Schiavon, E., T. Sacco, R.R. Cassulini, G. Gurrola, F. Tempia, L.D. Possani, and E. Wanke. 2006.
26 Resurgent current and voltage sensor trapping enhanced activation by a beta-scorpion toxin
27 solely in Nav1.6 channel. Significance in mice Purkinje neurons. *J. Biol. Chem.* 281:20326–
28 20337. doi:10.1074/jbc.M600565200.
- 29 Sheets, M.F., J.W. Kyle, R.G. Kallen, and D.A. Hanck. 1999. The Na channel voltage sensor
30 associated with inactivation is localized to the external charged residues of domain IV, S4.
31 *Biophys. J.* 77:747–757. doi:10.1016/S0006-3495(99)76929-8.
- 32 el-Sherif, N., H.A. Fozzard, and D.A. Hanck. 1992. Dose-dependent modulation of the cardiac sodium
33 channel by sea anemone toxin ATXII. *Circ. Res.* 70:285–301. doi:10.1161/01.RES.70.2.285.
- 34 Soderlund, D.M. 2010. State-Dependent Modification of Voltage-Gated Sodium Channels by
35 Pyrethroids. *Pestic. Biochem. Physiol.* 97:78–86. doi:10.1016/j.pestbp.2009.06.010.
- 36 Soderlund, D.M. 2012. Molecular mechanisms of pyrethroid insecticide neurotoxicity: recent
37 advances. *Arch. Toxicol.* 86:165–181. doi:10.1007/s00204-011-0726-x.
- 38 Song, J.H., and T. Narahashi. 1996. Modulation of sodium channels of rat cerebellar Purkinje neurons
39 by the pyrethroid tetramethrin. *J. Pharmacol. Exp. Ther.* 277:445–453.
- 40 Stadler, T., A.O. O'Reilly, and A. Lampert. 2015. Erythromelalgia Mutation Q875E Stabilizes the
41 Activated State of Sodium Channel Nav1.7. *J. Biol. Chem.* 290:6316–6325.
42 doi:10.1074/jbc.M114.605899.

- 1 Stevens, M., S. Peigneur, and J. Tytgat. 2011. Neurotoxins and Their Binding Areas on Voltage-Gated
2 Sodium Channels. *Front. Pharmacol.* 2. doi:10.3389/fphar.2011.00071.
- 3 Tabarean, I.V., and T. Narahashi. 1998. Potent modulation of tetrodotoxin-sensitive and tetrodotoxin-
4 resistant sodium channels by the type II pyrethroid deltamethrin. *J. Pharmacol. Exp. Ther.*
5 284:958–965.
- 6 Tabarean, I.V., and T. Narahashi. 2001. Kinetics of Modulation of Tetrodotoxin-Sensitive and
7 Tetrodotoxin-Resistant Sodium Channels by Tetramethrin and Deltamethrin. *J. Pharmacol.*
8 *Exp. Ther.* 299:988–997.
- 9 Tan, J., and D.M. Soderlund. 2010. Divergent Actions of the Pyrethroid Insecticides S-Bioallethrin,
10 Tefluthrin and Deltamethrin on Rat Nav1.6 Sodium Channels. *Toxicol. Appl. Pharmacol.*
11 247:229–237. doi:10.1016/j.taap.2010.07.001.
- 12 Tan, J., and D.M. Soderlund. 2011. Actions of Tefluthrin on Rat Nav1.7 Voltage-Gated Sodium
13 Channels Expressed in *Xenopus* Oocytes. *Pestic. Biochem. Physiol.* 101:21–26.
14 doi:10.1016/j.pestbp.2011.06.001.
- 15 Tatebayashi, H., and T. Narahashi. 1994. Differential mechanism of action of the pyrethroid
16 tetramethrin on tetrodotoxin-sensitive and tetrodotoxin-resistant sodium channels. *J.*
17 *Pharmacol. Exp. Ther.* 270:595–603.
- 18 Thull, S., C. Neacsu, A.O. O'Reilly, S. Bothe, R. Hausmann, T. Huth, J. Meents, and A. Lampert.
19 2020. Dataset of electrophysiological patch-clamp recordings of the effect of the compounds
20 deltamethrin, ATx-II and β 4-peptide on human cardiac Nav1.5 channel gating properties.
21 *Data in Brief*. Under Review.
- 22 Usherwood, P.N.R., T.G.E. Davies, I.R. Mellor, A.O. O'Reilly, F. Peng, H. Vais, B.P.S. Khambay,
23 L.M. Field, and M.S. Williamson. 2007. Mutations in DIIS5 and the DIIS4-S5 linker of
24 *Drosophila melanogaster* sodium channel define binding domains for pyrethroids and DDT.
25 *FEBS Lett.* 581:5485–5492. doi:10.1016/j.febslet.2007.10.057.
- 26 Vais, H., S. Atkinson, F. Pluteanu, S.J. Goodson, A.L. Devonshire, M.S. Williamson, and P.N.R.
27 Usherwood. 2003. Mutations of the para Sodium Channel of *Drosophila melanogaster* Identify
28 Putative Binding Sites for Pyrethroids. *Mol. Pharmacol.* 64:914–922.
29 doi:10.1124/mol.64.4.914.
- 30 Vais, H., M.S. Williamson, S.J. Goodson, A.L. Devonshire, J.W. Warmke, P.N. Usherwood, and C.J.
31 Cohen. 2000. Activation of *Drosophila* sodium channels promotes modification by
32 deltamethrin. Reductions in affinity caused by knock-down resistance mutations. *J. Gen.*
33 *Physiol.* 115:305–318.
- 34 Varga, Z., W. Zhu, A.R. Schubert, J.L. Pardieck, A. Krumholz, E.J. Hsu, M.A. Zaydman, J. Cui, and
35 J.R. Silva. 2015. Direct Measurement of Cardiac Na⁺ Channel Conformations Reveals
36 Molecular Pathologies of Inherited Mutations. *Circ. Arrhythm. Electrophysiol.* 8:1228–1239.
37 doi:10.1161/CIRCEP.115.003155.
- 38 Warmke, J.W., R.A.G. Reenan, P. Wang, S. Qian, J.P. Arena, J. Wang, D. Wunderler, K. Liu, G.J.
39 Kaczorowski, L.H.T.V. der Ploeg, B. Ganetzky, and C.J. Cohen. 1997. Functional Expression
40 of *Drosophila* para Sodium Channels : Modulation by the Membrane Protein TipE and Toxin
41 Pharmacology. *J. Gen. Physiol.* 110:119–133. doi:10.1085/jgp.110.2.119.
- 42 West, J.W., D.E. Patton, T. Scheuer, Y. Wang, A.L. Goldin, and W.A. Catterall. 1992. A cluster of
43 hydrophobic amino acid residues required for fast Na⁽⁺⁾-channel inactivation. *Proc. Natl.*
44 *Acad. Sci. U. S. A.* 89:10910–10914.

- 1 Xiao, Y., K. Blumenthal, and T.R. Cummins. 2014. Gating-Pore Currents Demonstrate Selective and
2 Specific Modulation of Individual Sodium Channel Voltage-Sensors by Biological Toxins.
3 *Mol. Pharmacol.* 86:159–167. doi:10.1124/mol.114.092338.
- 4 Yan, Z., Q. Zhou, L. Wang, J. Wu, Y. Zhao, G. Huang, W. Peng, H. Shen, J. Lei, and N. Yan. 2017.
5 Structure of the Nav1.4- β 1 Complex from Electric Eel. *Cell.* 170:470-482.e11.
6 doi:10.1016/j.cell.2017.06.039.
- 7 Yang, N., A.L. George, and R. Horn. 1996. Molecular Basis of Charge Movement in Voltage-Gated
8 Sodium Channels. *Neuron.* 16:113–122. doi:10.1016/S0896-6273(00)80028-8.
- 9 Zaydman, M.A., J.R. Silva, and J. Cui. 2012. Ion channel associated diseases: overview of molecular
10 mechanisms. *Chem. Rev.* 112:6319–6333. doi:10.1021/cr300360k.
- 11 Zhu, W., T.L. Voelker, Z. Varga, A.R. Schubert, J.M. Nerbonne, and J.R. Silva. 2017. Mechanisms of
12 noncovalent β subunit regulation of NaV channel gating. *J. Gen. Physiol.*
13 doi:10.1085/jgp.201711802.

1 **Figures and Legends**2 **Figure 1**

3 **Figure 1. Hooked sodium tail currents in Nav1.7 and Nav1.8 channels**

4 (a) Nav1.7 channels transfected to HEK293 cells. Representative current traces evoked by the
 5 indicated voltage protocol. Cells were treated with vehicle (black) and 1 μM deltamethrin (red) (b)
 6 Nav1.8 channels transfected to ND7 cells. Representative current traces evoked by the indicated
 7 voltage protocol. Cells were treated with vehicle (black) and 1 μM deltamethrin (red).
 8 The black arrow indicates tail currents of Nav1.7 or Nav1.8 treated with vehicle whereas the red
 9 arrow displays hooked tail currents induced by deltamethrin in Nav1.7 or Nav1.8 channels.

10 When recording fast gating Nav1.5 channels treated with 1 μM deltamethrin, we unexpectedly
 11 observed small hooked tail currents that resembled resurgent currents known from Nav channels in the
 12 central nervous system (Raman and Bean, 1997). Unlike typical resurgent currents, however, these
 13 resurgent-like currents of Nav1.5 were induced in the absence of an open-channel pore-blocker (Fig.
 14 2a, b) and did not increase with higher concentrations of deltamethrin (see Fig. 1 (Thull et al., 2020)).
 15 They merged quickly into large deltamethrin-induced persistent currents and were observed only at
 16 very negative voltages (between -120 mV and -90 mV). Compared to tail currents, which decay

1 exponentially directly after repolarization, deltamethrin-induced hooked, resurgent-like currents

2 showed a clearly detectable activation component and a relatively slow time-to-peak (Fig. 3).

3

1
2
3
4
5
6
7
8
9
10
11
12
13
14
15
16
17
18
19
20
21
22
23
24
25
26
27
28
29
30
31
32
33
34
35
36
37
38
39
40
41
42
43
44
45
46
47
48
49
50
51
52
53
54
55
56
57
58
59
60
61
62
63
64
65

Figure 2

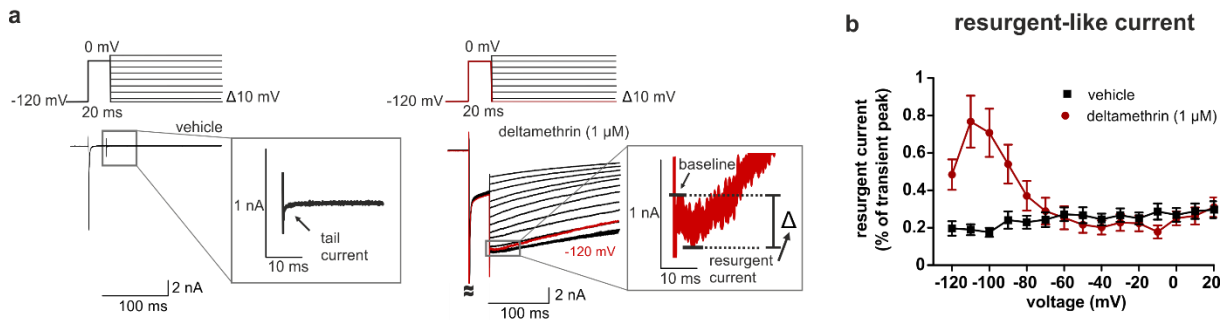


Figure 2. Nav1.5 channels display resurgent-like currents

(a) Representative current traces evoked by the indicated voltage protocol in human Nav1.5 channels expressed in HEK293 cells. Cells were treated with vehicle (left, black) and 1 μM deltamethrin (right, red). Magnified sections show the tail current in vehicle recordings and a resurgent-like current at -120 mV of 1 μM deltamethrin. Resurgent-like currents were determined as maximal current, elicited during repolarization, subtracted from a baseline. (b) Resurgent-like currents were normalized to maximum inward current of the depolarizing pre-pulse. Maximum resurgent-like currents were obtained at -110 mV: 1 μM deltamethrin 0.77 % ± 0.13 % (red, n = 15, mean AUC (-120 mV to -80 mV) 0.02 mV% ± 0.003 mV%), vehicle 0.19 % ± 0.03 % (black, n = 15, mean AUC (-120 mV to -80 mV) 0.01 mV% ± 0.002 mV%, p = 0.0005 vs. vehicle, difference between means = 0.01 mV% ± 0.003 mV%, 95% CI 0.006 mV% to 0.02 mV%, t-ratio = 3.9, unpaired t-test of the area under the curve (AUC) (-120 mV to -80 mV)).

Figure 3

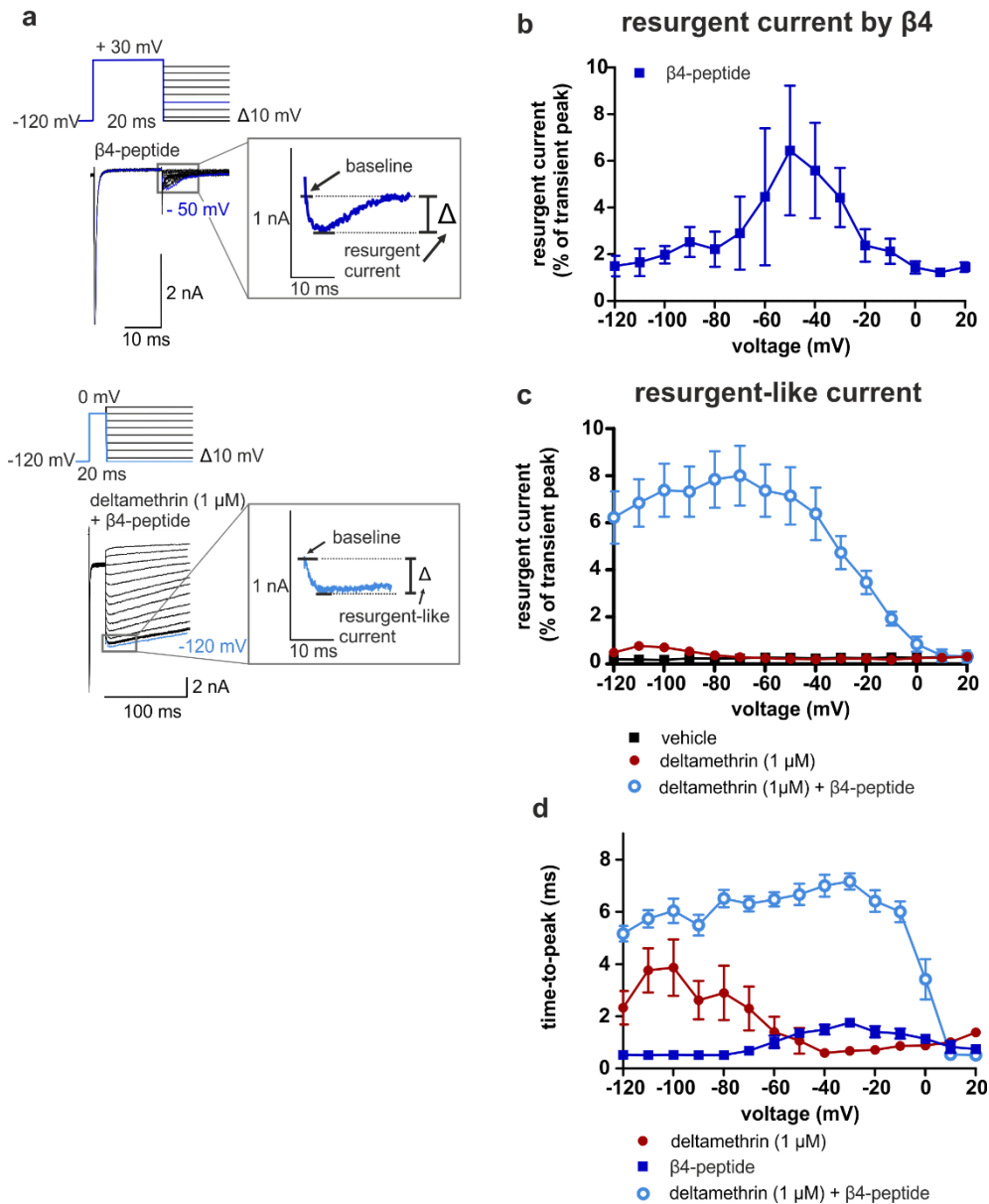


Figure 3. Deltamethrin and $\beta 4$ -peptide generate resurgent(-like) currents by a distinct mechanism

(a) Representative current traces evoked by the indicated voltage protocols in human Nav1.5 channels expressed in HEK293 cells. Cells were treated with 100 μM $\beta 4$ -peptide (top) and 1 μM deltamethrin + 100 μM $\beta 4$ -peptide (bottom). Magnified sections show representative traces of resurgent current at -50 mV with $\beta 4$ -peptide (top; dark blue) and at -120 mV with 1 μM deltamethrin + 100 μM $\beta 4$ -peptide (bottom; light blue). Resurgent-like currents were determined as in Fig 2. (b) $\beta 4$ -mediated resurgent currents, evoked and analyzed as in (a), using a pre-pulse to +30 mV. The intracellular recording solution contained 100 μM $\beta 4$ -peptide. Resurgent currents were normalized as described in Fig. 2b.

1 The maximum resurgent current was obtained at -50 mV ($6.44 \% \pm 3.78 \%$; $n = 8$). Resurgent currents
2 induced by the $\beta 4$ -peptide are much larger than deltamethrin-induced currents. Also note the different
3 voltage dependence of $\beta 4$ resurgent currents. (c) Resurgent-like currents, evoked by vehicle (black, n
4 = 16), 1 μ M deltamethrin (red, $n = 16$) or 1 μ M deltamethrin + 100 μ M $\beta 4$ peptide (blue, $n = 13$) as
5 in (a), using a pre-pulse to 0 mV. The red and black graphs are the same as in Fig. 2b and were
6 included for comparison. In contrast to individual deltamethrin and $\beta 4$ peptide treatments, resurgent-
7 like currents induced by the combination of both compounds are larger, appearing almost over the
8 entire voltage range. (d) Time-to-peak of the resurgent-like current in the different treatments.
9 Resurgent-like currents induced by deltamethrin are generally slower compared to $\beta 4$ resurgent
10 currents. The combination of both compounds increases the time-to-peak even further at most
11 voltages.

Figure 4

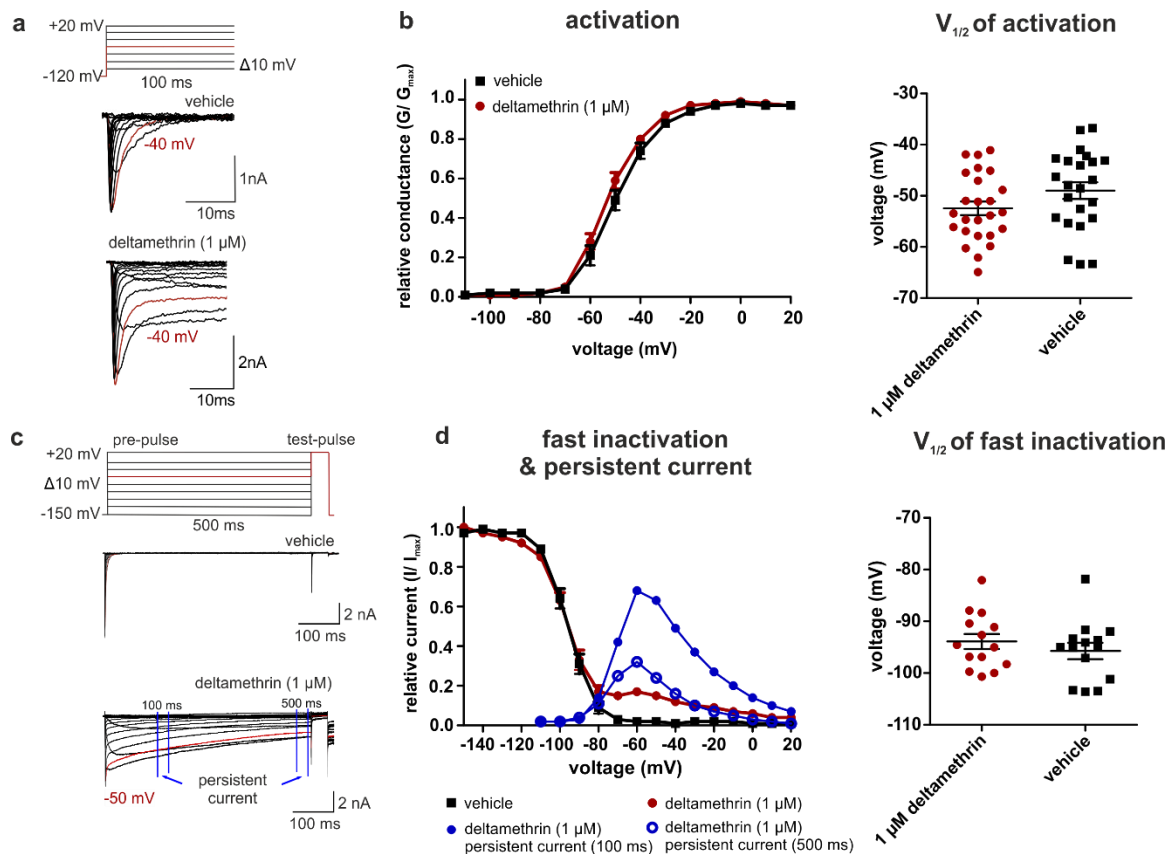


Figure 4. Deltamethrin does not affect the voltage dependence of activation and fast inactivation of Nav1.5

(a) Representative voltage protocol and current traces of activating sodium currents in vehicle or 1 μ M deltamethrin recordings of human Nav1.5 in HEK293 cells. (b) Conductance-voltage relationship of Nav1.5 in vehicle or 1 μ M deltamethrin. Values for half maximal voltage-dependent activation ($V_{1/2}$) obtained from Boltzmann fits are: 1 μ M deltamethrin -52.5 mV \pm 1.3 mV (red, $n = 14$); vehicle -49.0 mV \pm 1.6 mV (black, $n = 14$, $p = 0.1$ vs. deltamethrin, difference between means = 3.5 mV \pm 2.1 mV, 95% CI -0.7 mV to 7.7 mV, t -ratio = 1.7, unpaired t -test). (c) Representative voltage protocol and current traces of inactivating sodium currents in vehicle or 1 μ M deltamethrin recordings of human Nav1.5 in HEK293 cells. (d) Voltage dependence of steady-state fast inactivation measured using the voltage protocol in (c). Half-maximal inactivation ($V_{1/2}$) of vehicle recordings: -95.7 mV \pm 1.6 mV (black, $n = 14$), and of 1 μ M deltamethrin recordings: -93.9 mV \pm 1.5 mV (red, $n = 14$, $p = 0.4$ vs. vehicle, difference between means = 1.8 mV \pm 2.4 mV, 95% CI -2.6 mV to 6.2 mV, t -ratio = 0.9, unpaired t -test). Half-maximal inactivation of deltamethrin recordings shows no difference to vehicle

1 recordings. Mean persistent current of 1 μ M deltamethrin recordings was measured after 100 ms
2 (filled blue, $n = 16$) and after 500 ms of depolarizing pre-pulse (unfilled blue, $n = 16$).
3

4
5
6
7
8
9
10
11
12
13
14
15
16
17
18
19
20
21
22
23
24
25
26
27
28
29
30
31
32
33
34
35
36
37
38
39
40
41
42
43
44
45
46
47
48
49
50
51
52
53
54
55
56
57
58
59
60
61
62
63
64
65

Figure 5

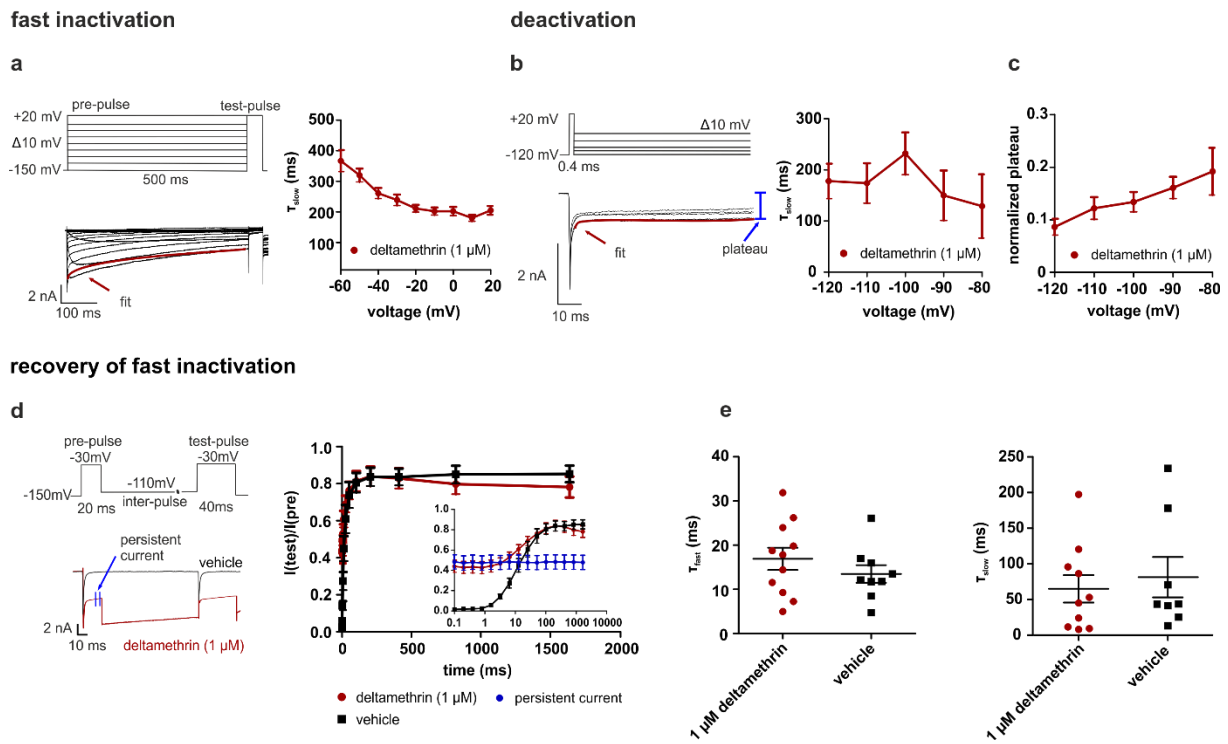


Figure 5. Deltamethrin slows fast inactivation and deactivation but does not affect recovery of fast inactivation of Nav1.5 channels

(a) Time course of persistent current decay during fast inactivation. Left: representative voltage protocol and traces of fast inactivation during 1 μ M deltamethrin recordings. For calculating the slow time course of persistent current decay, time constants were obtained by a double-exponential fit to the slow component of current decay over 500 ms (fit highlighted in red). The quickly inactivating component (see Fig. 2 (Thull et al., 2020)) was not included in the fit. Right: slow time constant (τ_{slow} ; $n = 16$) of persistent current decay. The fast time constant (τ_{fast}) is not displayed as it presumably represents a mixed population of deltamethrin bound and unbound channels. (b) Time course of persistent current decay during deactivation. Left: representative voltage protocol and traces of deactivation during 1 μ M deltamethrin recordings. Calculating the time course of persistent current decay was performed as described in (a) but fitting over 100 ms (fit highlighted in red). Right: slow time constant (τ_{slow} ; $n = 19$) of persistent current decay at deactivating voltages. (c) The fraction of persistent current remaining after 100 ms of deactivation was determined by the plateau of the double-exponential fit (blue arrow in b and Y_0 in function, see Methods). The plateau was normalized to the

1 maximum tail current. (d) Recovery of fast inactivation during vehicle (black) and 1 μ M deltamethrin
2 (red) treatment was measured by the indicated voltage protocol with varying inter-pulse durations.
3
4 3 Test-pulse current ($I(\text{test})$) was normalized to the corresponding pre-pulse current ($I(\text{pre})$) and plotted
5
6 4 against inter-pulse duration. Data were best fitted with a double-exponential function and either
7
8 5 depicted using a linear scale (right graph) or a logarithmic scale (inset). Mean persistent current
9
10 6 (inset, $n = 11$) is shown in blue. Below 10 ms inter-pulse duration, persistent current prevents analysis
11
12 7 of recovery. (e) Time course of recovery of fast inactivation represented by τ_{fast} : vehicle $13.5 \text{ ms} \pm 2.0$
13
14 8 ms (black, $n = 9$) and 1 μ M deltamethrin $16.9 \text{ ms} \pm 2.5 \text{ ms}$ (red, $n = 11$, $p = 0.3$, difference between
15
16 9 means = $3.4 \text{ ms} \pm 3.3 \text{ ms}$, 95% CI -3.6 ms to 10.4 ms , t -ratio = 1.0, no difference vs. vehicle, unpaired
17
18 10 t -test); and by τ_{slow} : vehicle $81.3 \text{ ms} \pm 28.3 \text{ ms}$ (black, $n = 9$) and 1 μ M deltamethrin $65.1 \text{ ms} \pm 19.3 \text{ ms}$
19
20 11 (red, $n = 9$, $p = 0.6$, difference between means = $16.2 \text{ ms} \pm 33.2 \text{ ms}$, 95% CI -54.2 ms to 86.6 ms , t -
21
22 12 ratio = 0.5, no difference vs. vehicle, unpaired t -test). Deltamethrin does not affect the time courses of
23
24 13 recovery from fast inactivation.
25
26
27
28
29
30
31
32
33
34
35
36
37
38
39
40
41
42
43
44
45
46
47
48
49
50
51
52
53
54
55
56
57
58
59
60
61
62
63
64
65

Figure 6

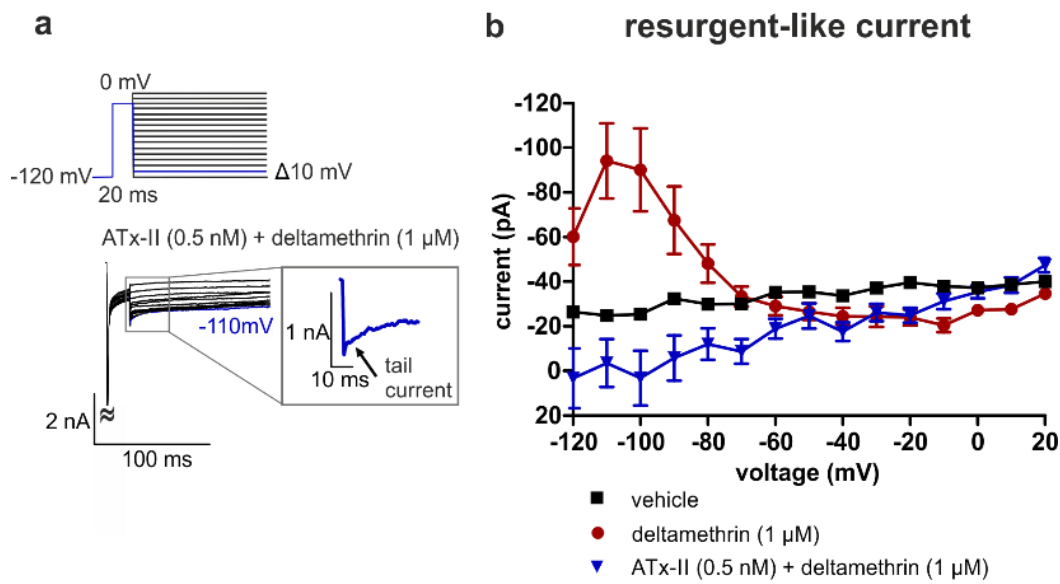


Figure 6. ATx-II prevents the generation of resurgent-like currents

(a) Representative currents evoked by the indicated voltage protocol in 0.5 nM ATx-II + 1 μM deltamethrin. The highlighted trace is magnified in the grey box, showing tail currents but no resurgent-like currents. (b) Resurgent-like currents, determined as described in Fig. 2a, during vehicle (black, n = 22), 1 μM deltamethrin (red, n = 19) or 1 μM deltamethrin + 0.5 nM ATx-II (blue, n = 11). To simplify comparison, the y-axis is inverted. The combination of ATx-II and deltamethrin does not generate resurgent-like currents.

Figure 7

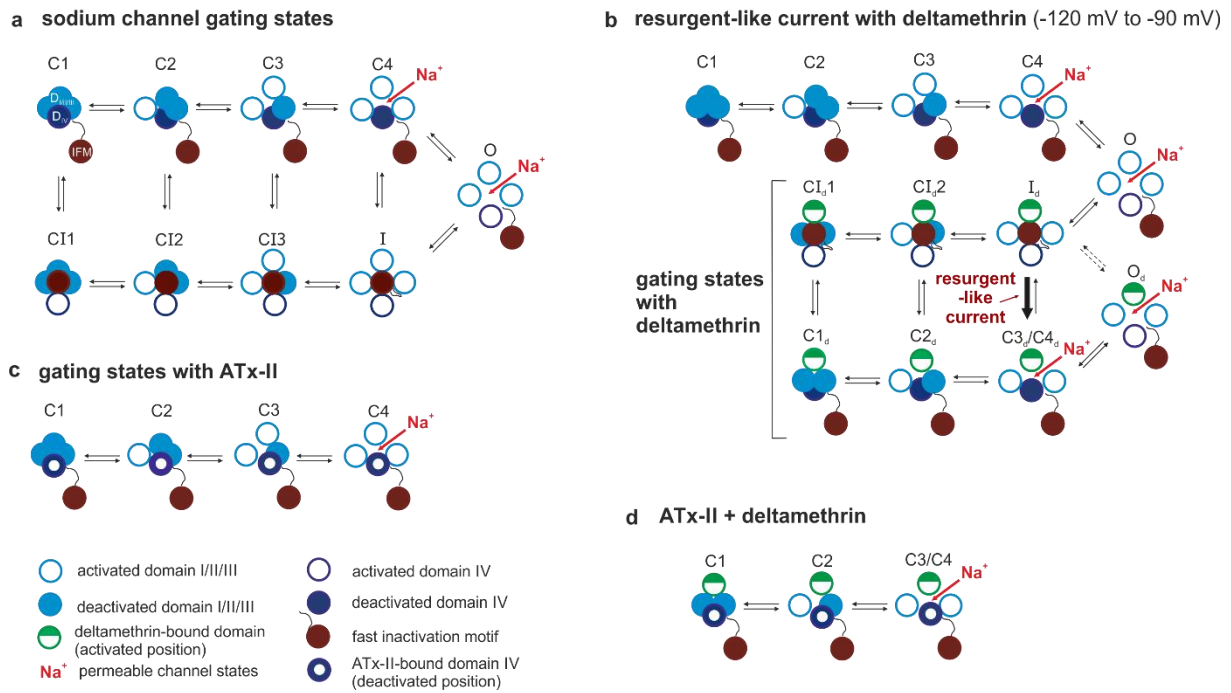


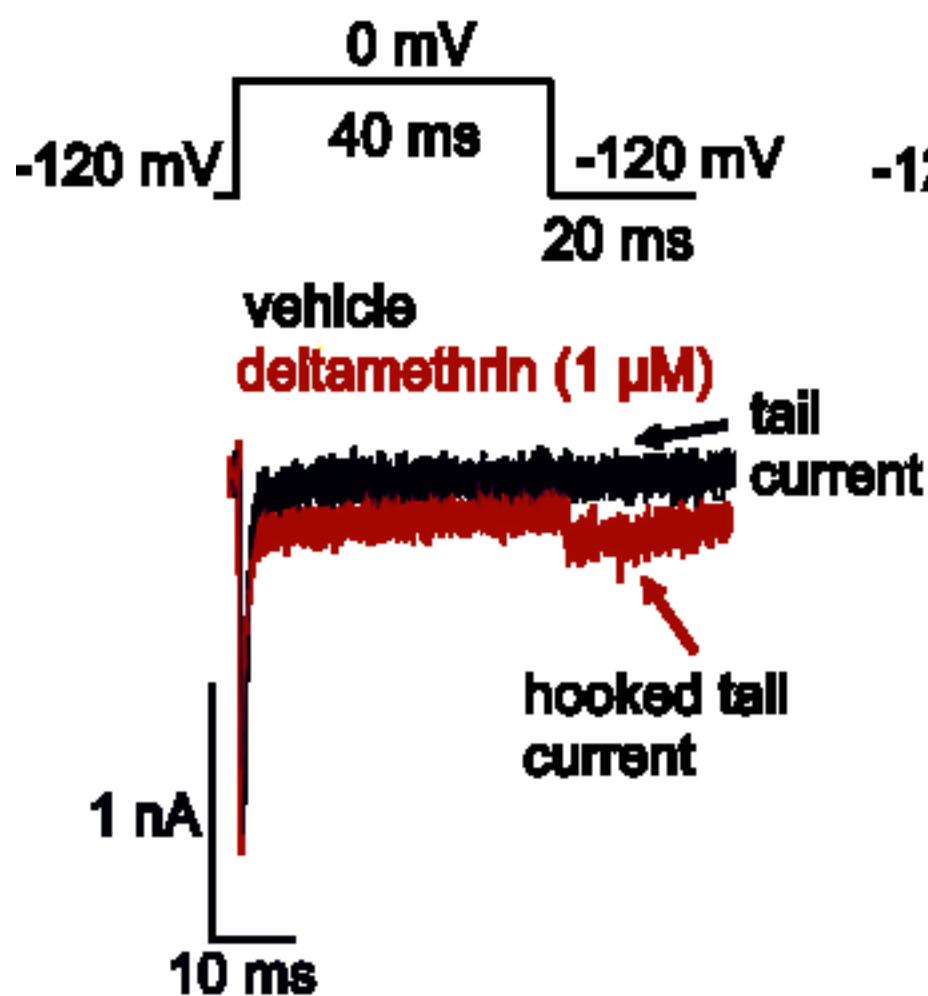
Figure 7. Deltamethrin produces resurgent-like currents by slowing deactivation

(a) Schematic display of gating states of human Nav1.5 channels. During activation, channels transition between closed states C1 to C4 with DI-III moving outward fast (unfilled light blue). Following activation, channels are permeable either with DIV still deactivated (filled dark blue) in state C4 or with DI-IV completely activated in state O. When DIV is activated (unfilled dark blue), channels quickly undergo fast inactivation and the inactivation particle (IFM, filled red) occludes the open pore (I). Upon repolarization with the inactivation particle bound, DI-III deactivate fast (filled light blue) (CI3-CI1). Accompanying the deactivation of DIV, the inactivation particle unbinds from the pore, returning the channel to state C1. (b) Schematic display of gating states of Nav1.5 channels treated by deltamethrin and producing resurgent-like currents. We propose that resurgent-like currents only occur in channels that bind deltamethrin after having undergone fast inactivation. Therefore, the first gating states that occur during channel activation (C1-C4-O-I) are analogous to (a). Once the inactivated channel has bound deltamethrin, DII (white-green) is stabilized in its activated position. Thus, gating states C3 and C4 become identical and permeable (C_d3/C_d4). Bold arrow indicates the transition that may lead to resurgent-like currents: As deltamethrin slows channel deactivation, recovery from fast inactivation (I_d-C_d3/C_d4) may precede deactivation and briefly return

1 the channel to a conductive state. Fast inactivation of deltamethrin-bound channels (O_d-I_d) is slowed
2 (dashed arrows), leading to large persistent currents. (c) Schematic display of gating states of Nav1.5
3 channels treated by ATx-II. Activation of DIV (open dark blue) is inhibited, preventing the binding of
4 the fast inactivation particle to the open channel pore. Only gating state C4 is therefore conductive. In
5 this theoretical model, states O, I and CI do not exist. (d) Schematic display of gating states of Nav1.5
6 channels treated by ATx-II and deltamethrin. DII (white-green) is stabilized in its activated position by
7 deltamethrin as in (b). Activation of DIV (open dark blue) is inhibited by ATx-II and prevents fast
8 inactivation as in (c). C3/C4 is permeable. In this theoretical model, states O, I and CI do not exist.
9 In this simplified overview, possible additional states and transitions between depicted states are not
10 captured but may occur. Channel states: C closed, O open, I inactivated, CI closed-inactivated; a
11 subscript _a indicates a deltamethrin-bound state. See main text for further details.

Figure 1

a Nav1.7



b Nav1.8

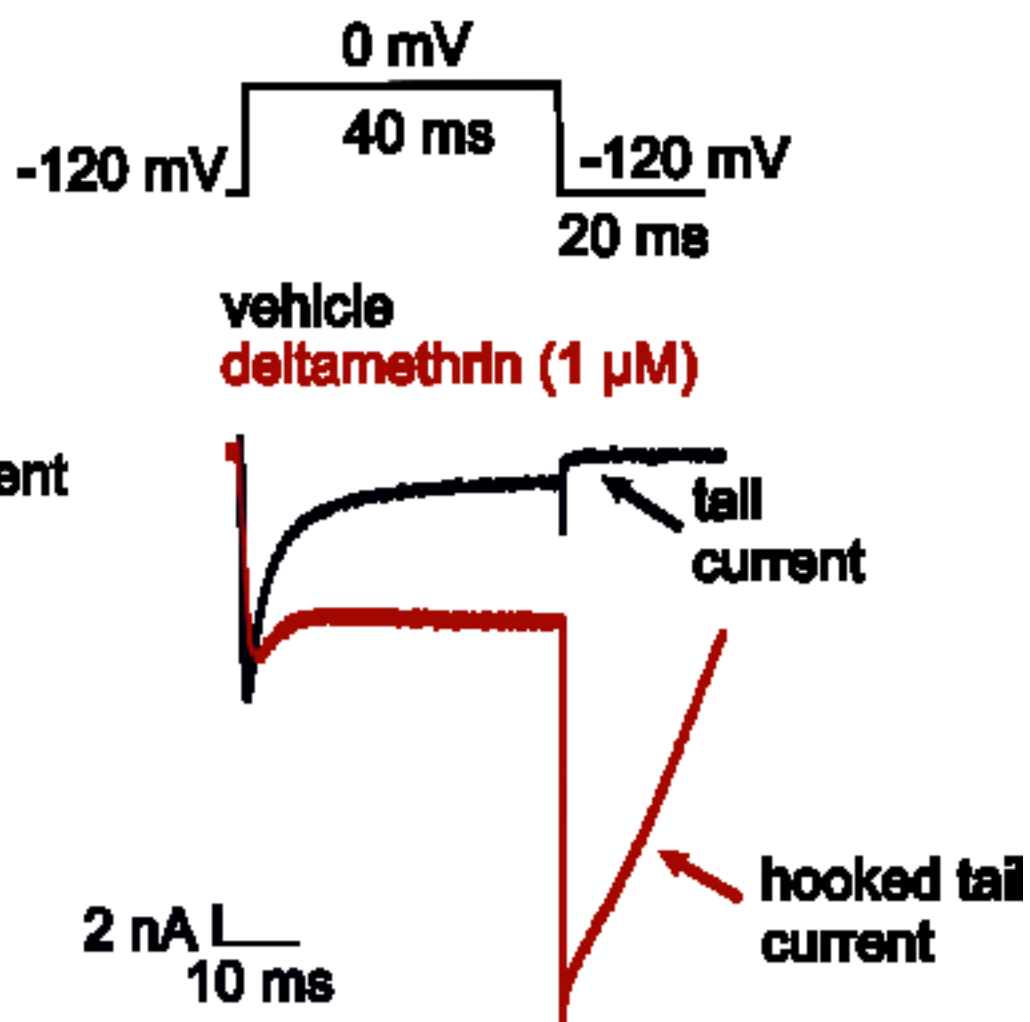


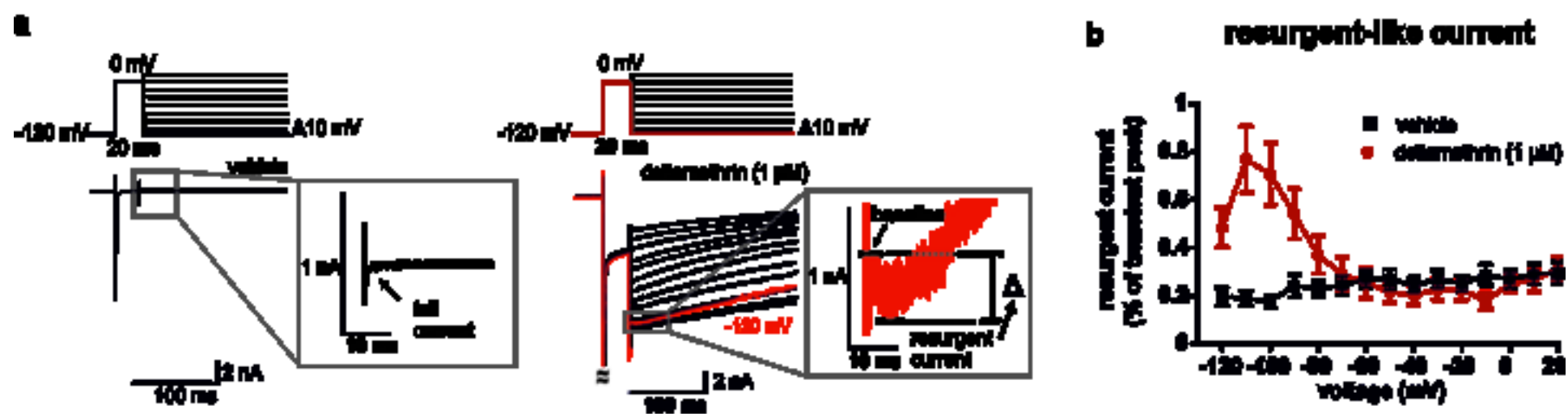
Figure 2

Figure 3

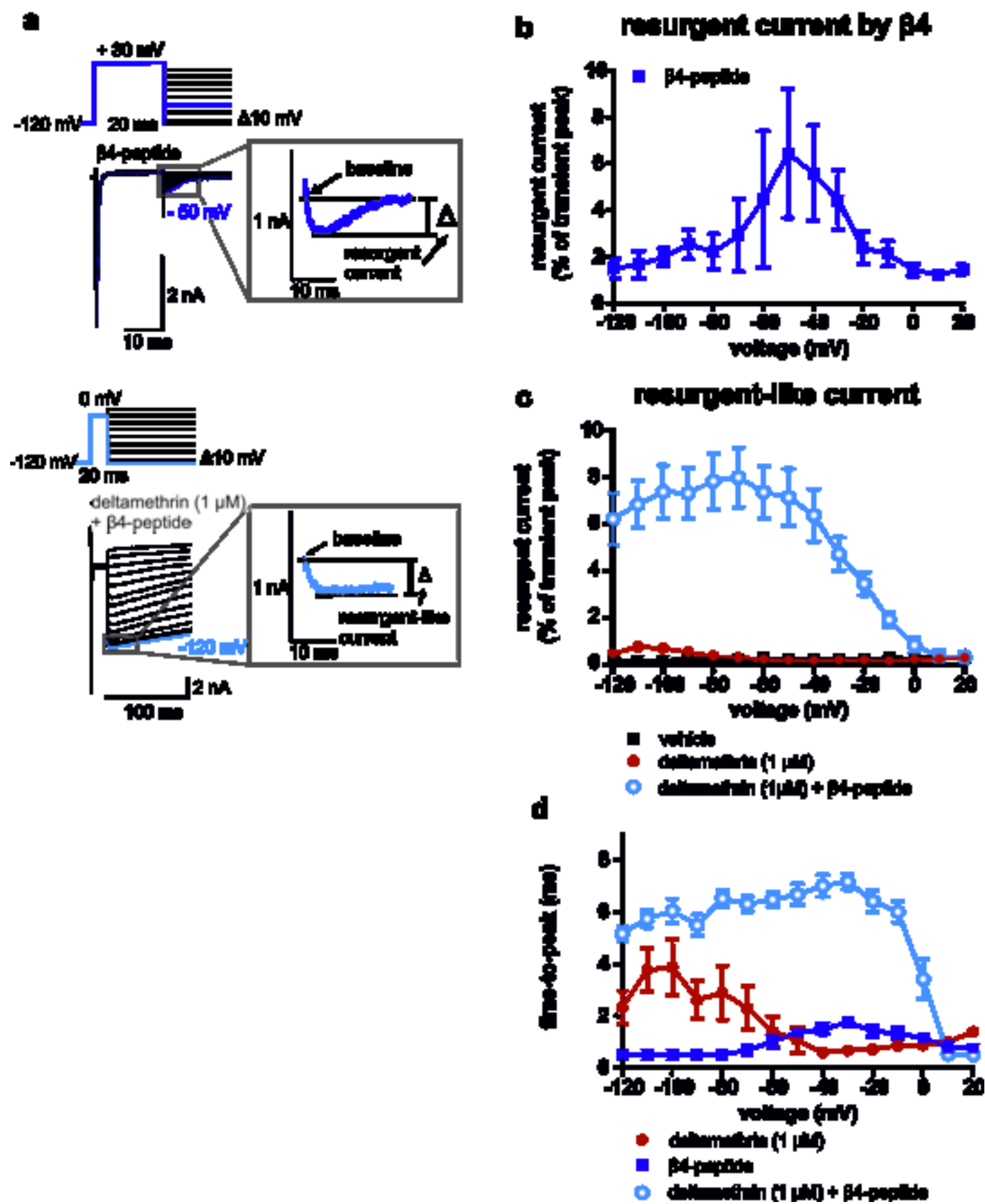


Figure 4

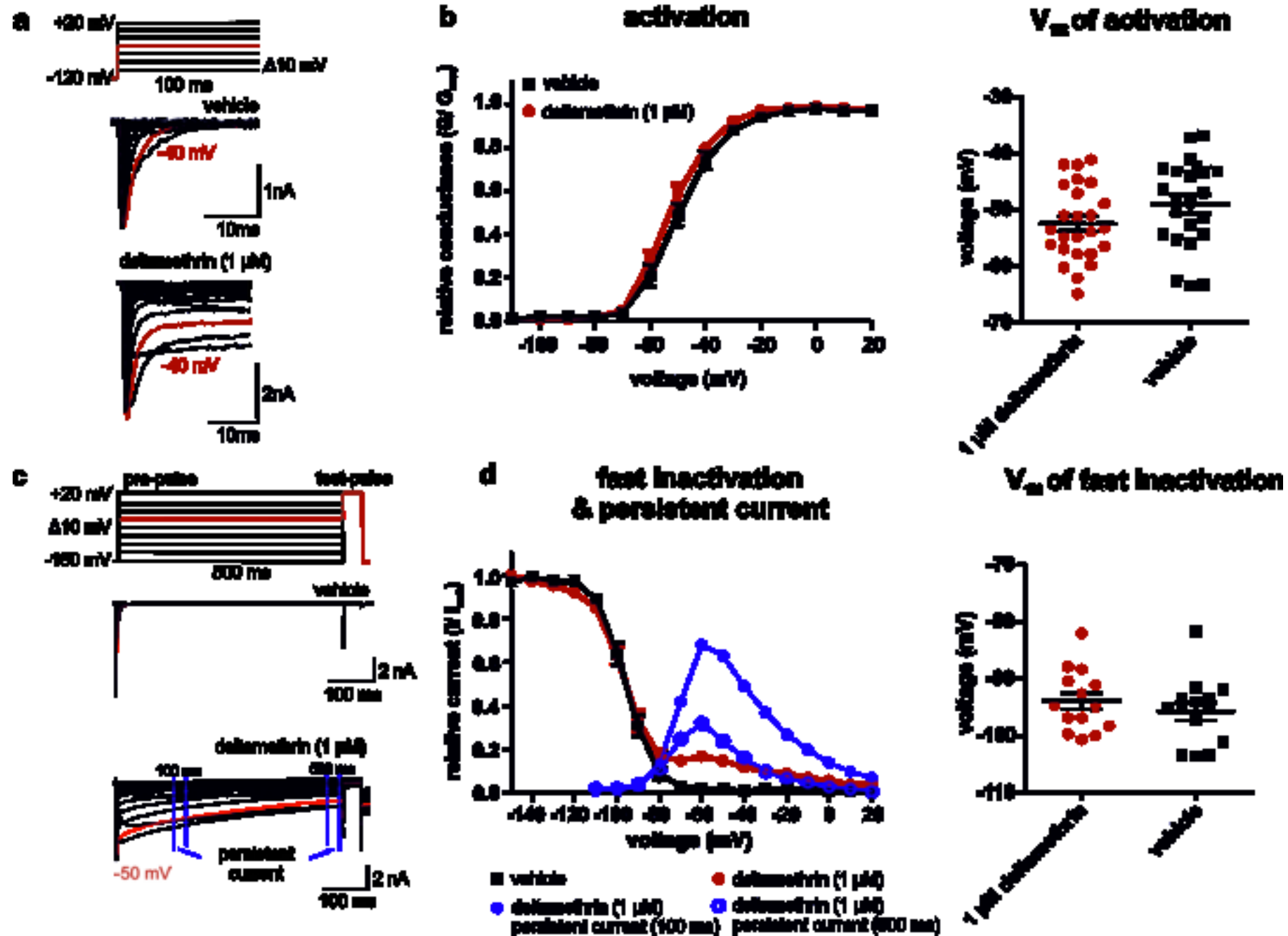
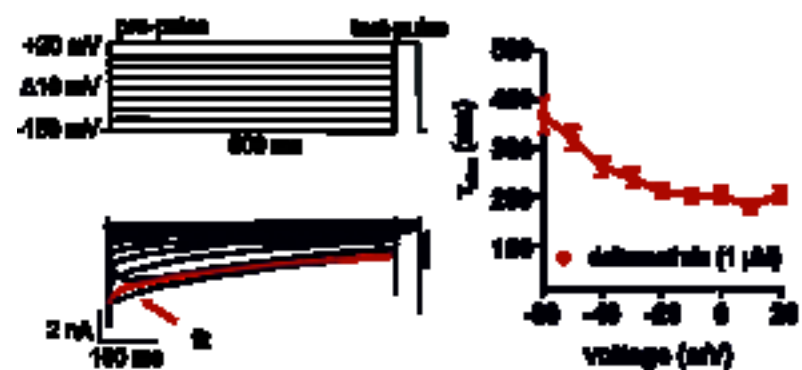


Figure 5

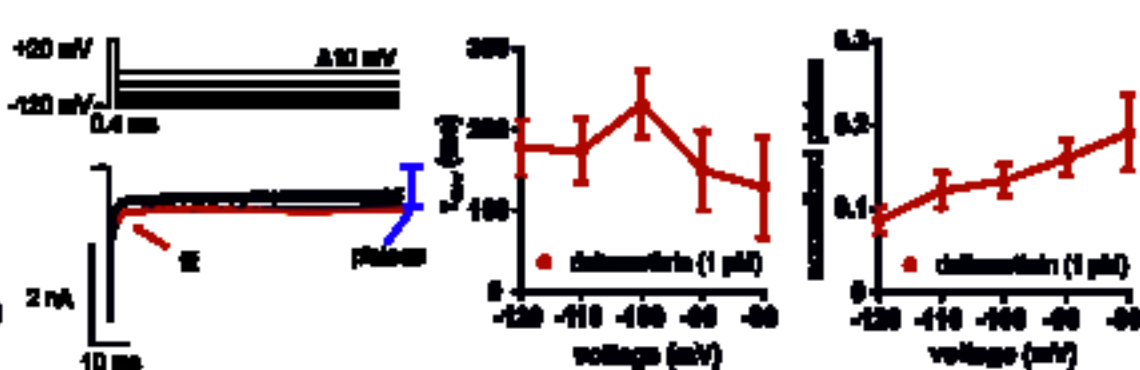
fast inactivation

a



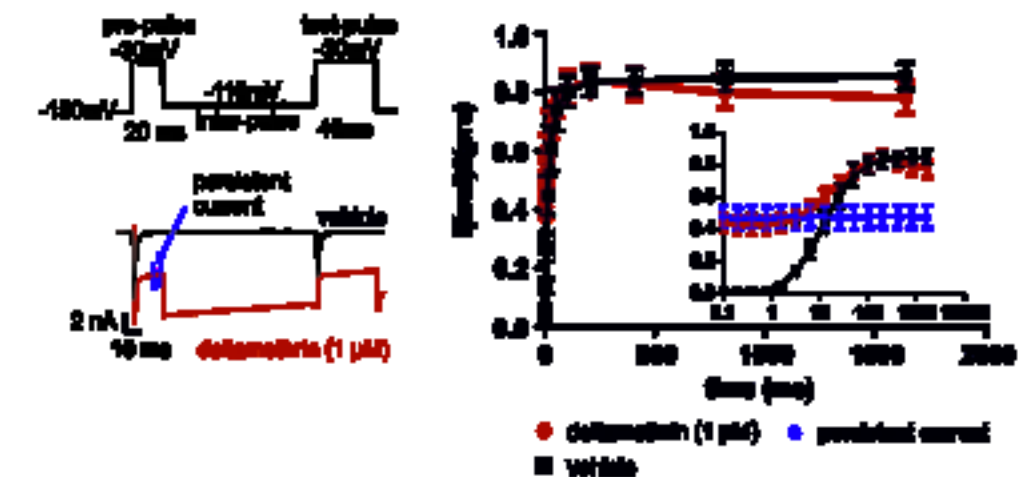
deactivation

b



recovery of fast inactivation

d



e

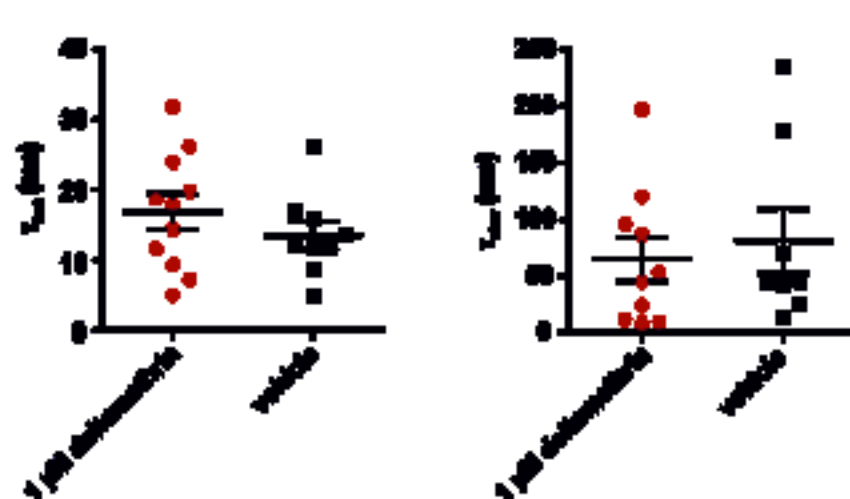


Figure 6

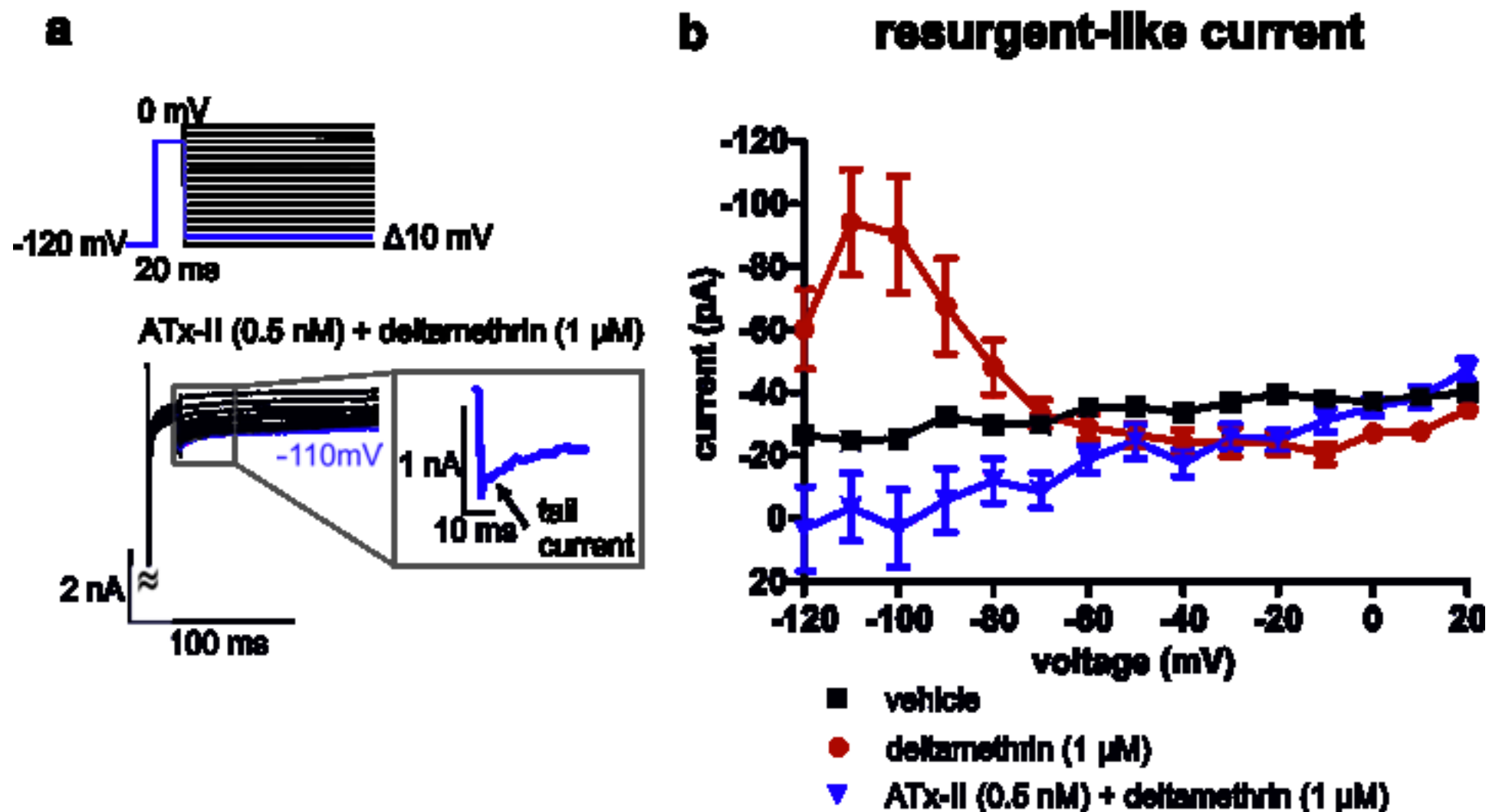
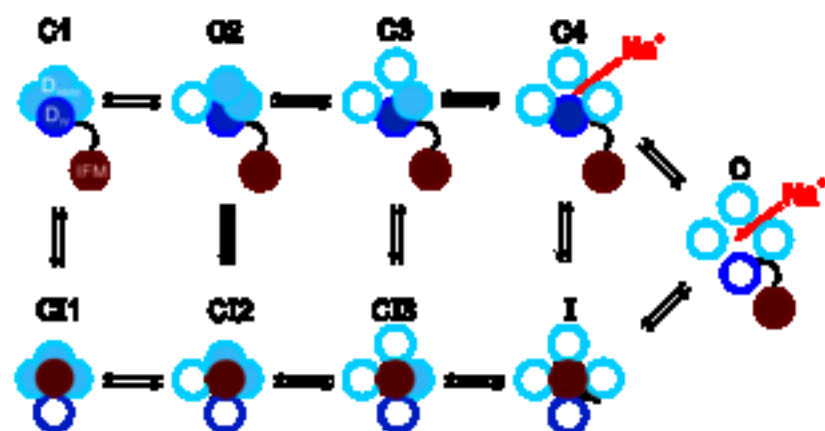
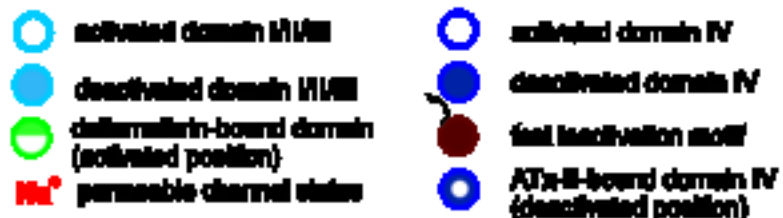
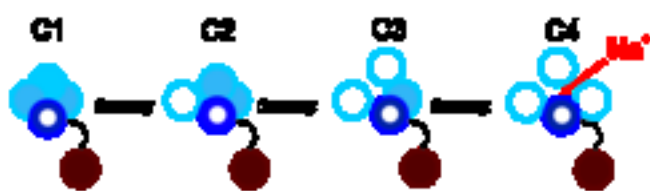


Figure 7

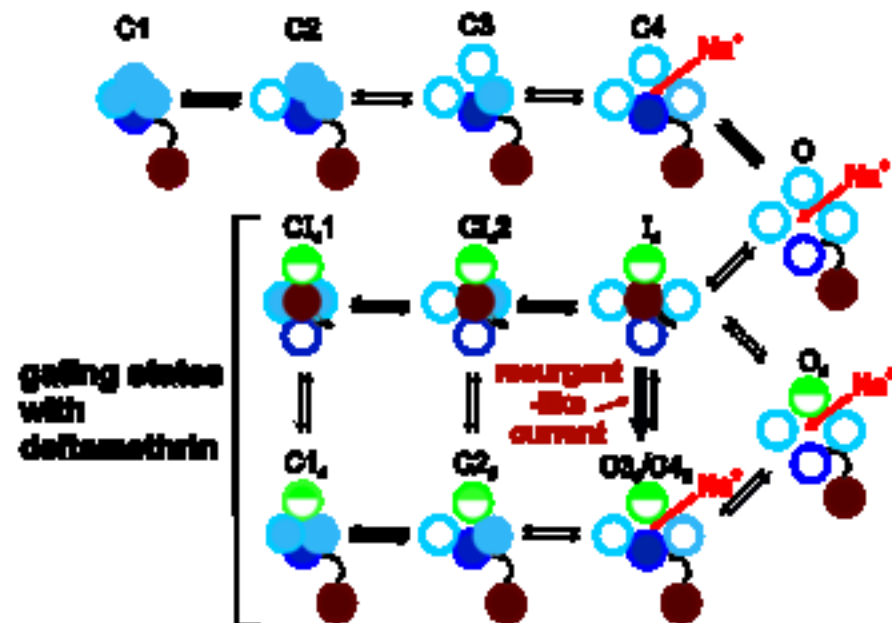
a sodium channel gating states



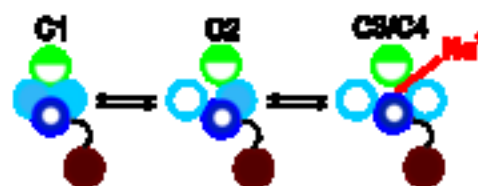
b gating states with ATx-II



b reurgent-like current with deltamethrin (-120 mV to -80 mV)



d ATx-II + deltamethrin



Data in Brief

[Click here to download Data in Brief: Data in Brief Thull.zip](#)